including artifacts and were excluded from further analysis [51]. Source imaging of MEG data in the time–frequency domain was performed using the multiple source beamformer (MSBF) implemented in Brain Electrical Source Analysis (BESA) software (Fig. 2). The MSBF is a modified version of the linearly constrained minimum variance vector beamformer in the time–frequency domain [52]. As an adaptive beamformer, the MSBF applies a spatial filter specific for each brain voxel that is fully sensitive to activity from the target voxel, while being as insensitive as possible to activity from other brain regions, thus suppressing interference from unwanted signals. We analyzed frequencies between 1 and 60 Hz in 2-Hz steps; latencies were sampled in steps of 25 ms. The BESA beamformer applied complex demodulation to transform time-domain MEG data into time–frequency data. This provided information on the envelope amplitude and the phase of a specified frequency band as a function of time [51,53]. The complex demodulation consisted of a multiplication of the time-domain signal by a complex periodic potential function with a frequency equal to the frequency analyzed and an additional low-pass filter. This low-pass filter was a Gaussian-shape finite impulse response filter in the time domain, which is related to the envelope of the moving window in wavelet analysis. In the resulting complex signal, its magnitude corresponded to half the envelope amplitude and its phase to the compound phase of the filtered frequency band. To obtain power values, the time-series MEG data were squared and averaged across all 20 trials. Time–frequency representations of changes in power normalized to baseline for each MEG sensor were obtained from each subject. An increase in power at a specific frequency compared with the mean power of the baseline period for that frequency was defined as event-related synchronization (ERS), whereas a decrease in power was deemed event-related desynchronization (ERD). Power changes displayed on a spectrogram are shown as percentages of ERS/ERD with color-coded intensities; the *x* axis and *y* axis relay the time relative to the "START" cue and the frequency, respectively (Fig. 2a). For each trial, a 2-second interval before the memory set (time window: 1–3 seconds after the "START" cue) was deemed baseline, and a 2-second interval after the memory set (time window: 6–8 seconds after the "START" cue) was deemed target interval (memory retention period) (Fig. 1). Source-power changes (ERD/ERS) were measured in five frequency bands: delta (1–4 Hz), theta (4–8 Hz), alpha (8–13 Hz), beta (13–30 Hz), and gamma (30–60 Hz). The alpha band was additionally subdivided into alpha1 (8–10 Hz) and alpha2 (10–13 Hz).

2.5.2. Statistical group analysis

To image induced oscillatory activity, BESA (www.besa.de) computed the complex cross-spectral density matrices (the time–

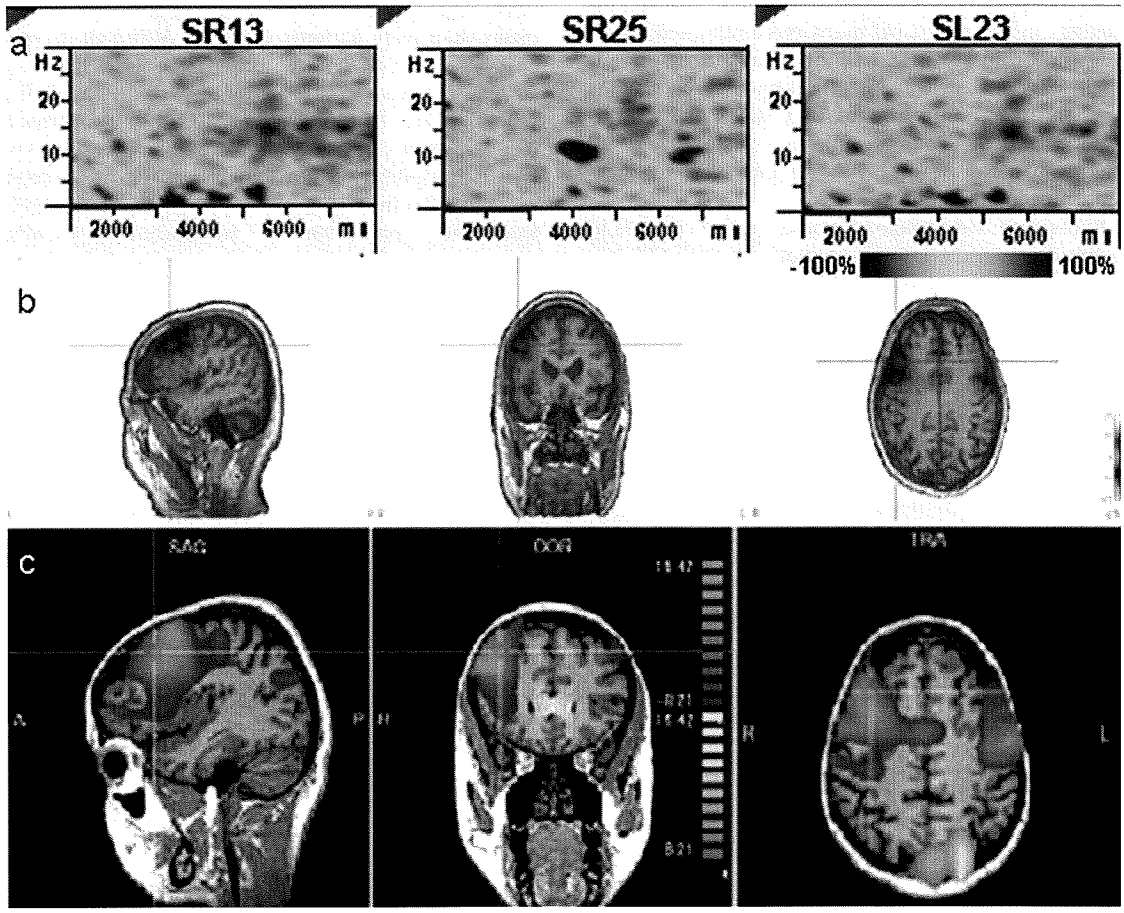

Fig. 2. Schematic representation of the time–frequency analysis. (a) Time–frequency plots for MEG channels showing power changes (averaged across all trials) in the alpha band (8–13 Hz) in a representative patient with chronic interictal psychosis. In the spectrogram, the *x* axis denotes the time relative to the "START" cue (ms), and the *y* axis denotes the frequency of oscillatory activity (Hz). Sustained event-related desynchronization (ERD) is observed in the 6- to 8-second time window (target interval) in channels overlying the right (SR13) and left (SL23) dorsolateral prefrontal cortex (DLPFC). A strong event-related synchronization (ERS) is observed in the target interval in the SR25 channel, which overlies the midline parietal region. (b) Multiple source beamformer (MSBF) analysis using BESA software. Color-coded maps show the magnitude change in the target interval relative to baseline as a percentage for the analyzed frequency band (alpha). (c) Brain Voyager image of source-power changes. The resulting beamformer three-dimensional images are exported to Brain Voyager QX and superimposed onto a T1-weighted brain template for group statistics. The color bars represent the percentages of decrease (blue/green, ERD) and increase (red/yellow, ERS) in oscillatory activity power changes. (For interpretation of the references in color in this figure legend, the reader is referred to the web version of this article.)

frequency equivalent of the data covariance matrix) for the target and baseline intervals from single-trial data for each frequency band of interest. Color-coded maps were obtained displaying q values as a measure of the magnitude change in the target interval relative to the baseline in percent (Fig. 2b). The beamformer three-dimensional images superimposed onto the BESA standard anatomical magnetic resonance image reveal locations of the generators of the induced oscillatory activity in the specified frequency. These images were exported for further statistical analysis to the Brain Voyager QX software package (Brain Innovation, Maastricht, The Netherlands) to assess between-group differences in source-power changes for each frequency band (Fig. 2c). BrainVoyager QX, originally developed for fMRI analysis [54], was used for group analysis of MEG data [55]. The subject's three-dimensional images of source-power changes were superimposed onto a Talairach-transformed Montreal Neurological Institute (MNI) T1-weighted brain template in Brain Voyager, and the anatomical T1 coordinates in the statistical maps were transformed into Talairach coordinates to identify brain regions with significant between-group differences in source-power changes. Between-group comparisons of brain activation patterns, as indicated by ERD/ERS values in a given frequency band, were based on t-test statistics (two-tailed, unpaired) in BrainVoyager QX. For correlation of neural activity in psychotic patients with external clinical variables, particularly medication dosage, the coordinates at the voxel with t_{maxima} (peak ERD/ERS value) at locations with significant power changes in the statistical maps were obtained. Then, the value at these coordinates in each individual's three-dimensional functional image for each one of the frequency bands was determined for analysis. To minimize the risk of false-positive findings, all activation foci were set to a minimum cluster size of 20 voxels [56], and statistical results with an uncorrected P value < 0.001 were considered significant.

To test our hypothesis, we compared source-power changes in oscillatory activity across three groups: (1) patients with CIP versus patients with nPE, (2) patients with schizophrenia versus healthy controls, and (3) patients with CIP versus those with schizophrenia. Analysis of groups 1 and 2 focused on patterns of WM dysfunction, whereas analysis of group 3 tested whether CIP and schizophrenia differed in functional cognitive abnormalities. Correlation analyses were carried out using Pearson's correlation coefficient to examine the association of medication dose with peak ERD/ERS values at sources with significant power changes in a given frequency band in patients with CIP and schizophrenia. The χ^2 test was performed for independence of group and gender. Demographic and clinical variables were analyzed using an unpaired two-tailed t test or ANOVA, with the significance level set at $P < 0.05$. Results are expressed as means ± SD. These statistical analyses were carried out using SPSS software (SPSS, Inc., Chicago, IL, USA).

3. Results

The clinical and demographic information of patients with CIP, nPE, and schizophrenia and of healthy controls is given in Table 1. There were no significant differences between the epilepsy groups (CIP vs nPE) with respect to age at epilepsy onset, duration, or seizure frequency. The majority of these patients had temporal lobe epilepsy (left $N = 10$, right $N = 10$, bilateral $N = 2$); only four patients (two in each group) had a diagnosis of frontal epilepsy. The patients with epilepsy were taking mainly carbamazepine or valproic acid. Approximately two-thirds of these patients ($N = 16$, 61.5%) were on monotherapy (CIP: $N = 5$, 41.7%; nPE: $N = 11$, 78.6%), and two patients in the CIP group were drug free. There were no between-group differences in plasma levels of these drugs. All patients with CIP had chronic interictal psychosis with onset 14.8 ± 8.6 years after the epilepsy. Comparison between the psychotic groups (CIP vs schizophrenia) revealed no significant difference in age at psychosis onset, although patients with schizophrenia presented with slightly longer psychosis duration. The analysis of chlorpromazine equivalents showed that patients with schizophrenia were taking higher doses of antipsychotic drugs than were patients with CIP. Although there was no difference in education across groups, post hoc ANOVA with Bonferroni correction revealed that patients with CIP, as well as those with schizophrenia, had lower IQs than healthy controls ($p < 0.005$ and 0.003, respectively); no significant differences in IQ were found between the epilepsy groups (CIP vs nPE) or the psychosis groups (CIP vs schizophrenia). Patients with schizophrenia and healthy controls did not differ in premorbid (preschizophrenia) IQ ($t[26] = -0.07$, $P = 0.94$), as assessed with JART.

3.1. Behavioral data

All subjects achieved an accuracy rate of 75% or higher on the WM task. Using ANOVA we found a significant difference in the correct-response percentage across groups ($F = 5.35$, $P = 0.003$), with patients with CIP performing worse (90.5 ± 7.1%) than those with nPE (96.7 ± 1.7%, $P = 0.013$) and healthy controls (97.4 ± 2.8%, $P = 0.004$). However, the psychosis groups did not differ in correct-response percentage (schizophrenia: 94.1 ± 6.0%, $P = 0.367$) (Fig. 3). Reaction times also significantly differed across

Table 1
Demographic and clinical data[a].

Characteristic	nPE ($N = 14$)	CIP ($N = 12$)	SCZ ($N = 14$)	HC ($N = 14$)	P
Age	33.6 ± 12.2	34.8 ± 12.7	34.9 ± 10.2	34.2 ± 11.3	0.99
Gender (F/M)	10/4	8/4	9/5	9/5	—
Education, years	14.4 ± 2.1	13.5 ± 2.4	14.2 ± 1.8	15.1 ± 1.8	0.23
WAIS-R IQ	99.1 ± 13.4	94.2 ± 7.0[b]	94.2 ± 11.8[b]	109.6 ± 10.5	0.002
Premorbid IQ			100.6 ± 9.4	101.2 ± 24.8	0.94
Epilepsy onset, years	20.4 ± 11.6	14.8 ± 12.2			0.25
Epilepsy duration, years	13.1 ± 10.1	18.5 ± 9.8			0.19
Seizure frequency/year	6.4 ± 10.2	11.1 ± 18.6			0.42
Epilepsy type (TLE/FLE)	12/2	10/2			0.88
CBZ plasma levels, μg/mL	5.7 ± .9.1	6.9 ± 3.0			0.37
VPA plasma levels, μg/mL	61.5 ± 35.9	44.0 ± 24.9			0.28
CPZ equivalents		341.7 ± 387.0	1021.9 ± 806.4		0.015
Psychosis onset, years		29.6 ± 14.9	20.3 ± 4.5		0.062
Psychosis duration, years		5.2 ± 4.3	14.6 ± 11.6		0.013

[a] Data are means ± SD unless otherwise noted. nPE, nonpsychotic epilepsy; CIP, chronic interictal psychosis; SCZ, schizophrenia; HC, healthy controls, WAIS-R, Wechsler Adult Intelligence Scale—Revised; TLE, temporal lobe epilepsy; FLE, frontal lobe epilepsy; CBZ, carbamazepine; VPA, valproic acid; CPZ, chlorpromazine.
[b] Significant difference relative to HC (post hoc ANOVA).

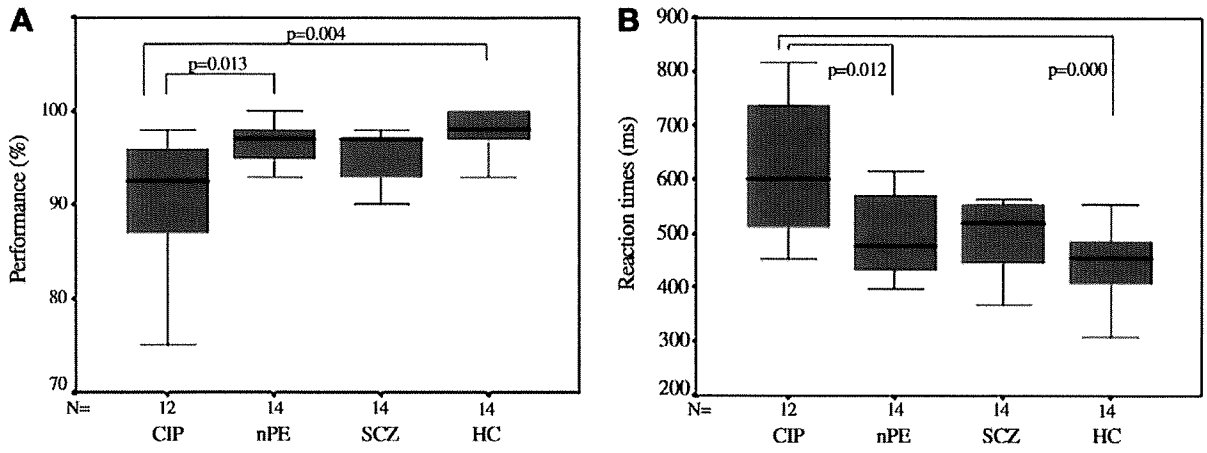

Fig. 3. Behavioral performance data as box plots. (A) Percentage of accurate response. (B) Reaction times. The boxes represent interquartile ranges. The whiskers show the highest and lowest values, excluding outliers. The lines across the boxes indicate medians. CIP, chronic interictal psychosis; nPE, nonpsychotic epilepsy; SCZ, schizophrenia; HC, healthy controls.

groups ($F = 7.15$, $P < 0.001$). The psychosis groups did not differ in reaction times (CIP: 619 ± 134 ms; schizophrenia: 519 ± 103 ms, $P = 0.066$), but patients with CIP had significantly longer reaction times compared with patients with nPE (495 ± 75 ms, $P = 0.012$) and healthy controls (448 ± 64, $P < 0.001$), as indicated by post hoc ANOVA with Bonferroni correction.

3.2. Power change analysis

We averaged the ERD/ERS percentages in different frequency bands and superimposed the data on a standard brain image (Fig. 4). This revealed that pronounced source-power changes exceeding 10% occurred only in alpha and theta frequency bands,

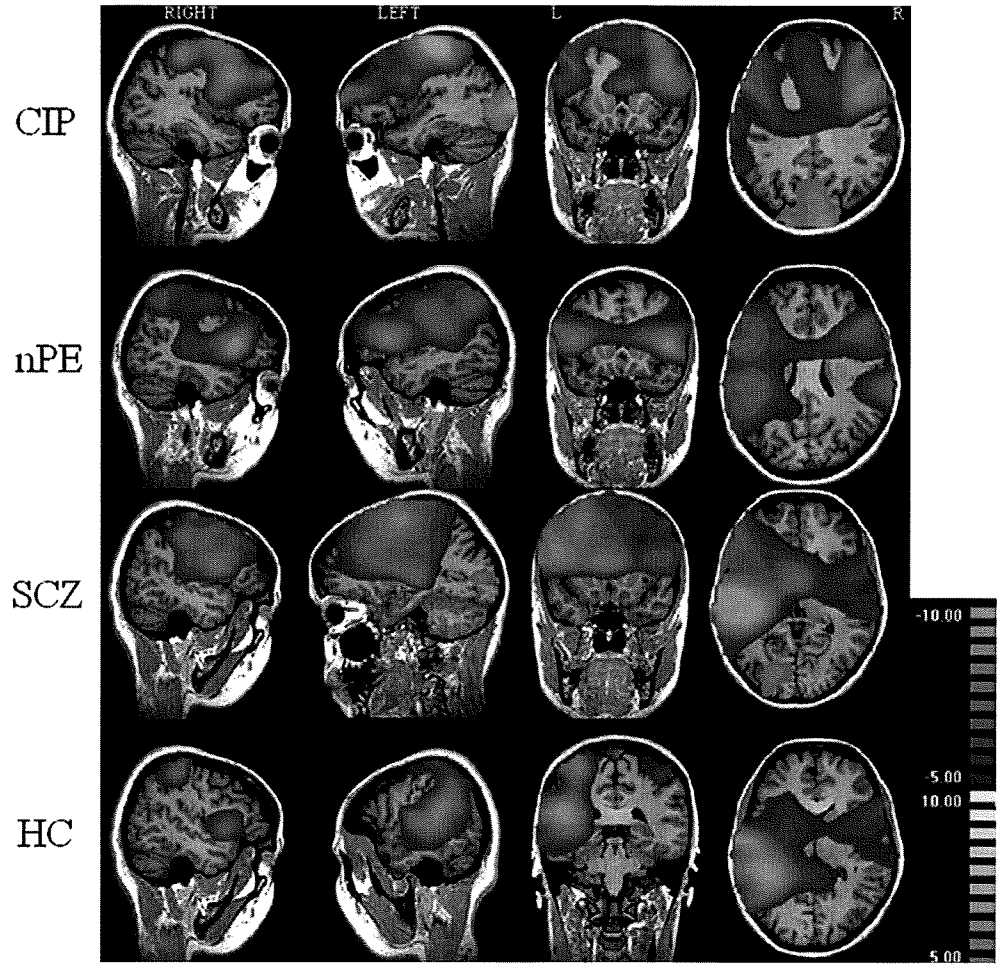

Fig. 4. Averaged alpha event-related desynchronization (ERD) and synchronization (ERS) greater than 5% across all groups using Brain Voyager. The color bars represent the percentages of decrease (blue/green, ERD) and increase (red/yellow, ERS) in oscillatory activity power changes. L, left; R, right; CIP, chronic interictal psychosis; nPE, nonpsychotic epilepsy; SCZ, schizophrenia; HC, healthy controls. (For interpretation of the references in color in this figure legend, the reader is referred to the web version of this article.)

particularly as ERD during WM retention. The alpha power was reduced bilaterally by 11.8% in the central-parietal regions and 11.5% in the right DLPFC, particularly over the superior frontal gyrus in patients with CIP. In patients with nPE, peak-averaged alpha ERD values >10% were only observed bilaterally in the DLPFC over the inferior frontal cortex (right: 10.7%, left: 10.3%) and bilaterally in the parietotemporal cortex (right: 10.2%; left: 10.8%).

In the theta frequency band, peak-averaged ERD > 10% was observed in patients with CIP over the right medial prefrontal and right parietal areas; this was not seen in patients with nPE (peak-averaged theta ERD 8.4%). In both patients with schizophrenia and healthy controls, peak-averaged alpha ERD values >10% were noted in central-parietal regions (schizophrenia: 15%; controls: 13%). In addition, there was pronounced ERD in the DLPFC (peak value: 11%) and in medial areas (peak value: 10.8%) in patients with schizophrenia and in the posterior temporal cortex in the controls (12.5%). Peak-averaged alpha ERD in the DLPFC was smaller than 8.5% in control subjects. Pronounced theta ERD was observed in parietal regions, predominantly on the left side (peak value: 12%) in patients with schizophrenia. At a threshold of 5% of power changes, alpha ERS was observed in patients with CIP and schizophrenia, but not in patients with nPE and healthy controls. This increase in alpha power occurred over posterior regions, particularly in medial parietal-occipital (peak value: 8.4%) and left posterior temporal (peak value: 7.7%) cortices in patients with CIP, and in the left temporal–occipital cortex (peak value: 6.7%) in patients with schizophrenia.

3.3. Between-group differences in source-power changes

The analysis of source-power changes in brain oscillatory activity during the retention period of the WM task between patients with CIP and those with nPE indicated significant differences in alpha frequency band: patients with CIP showed ERD in the right DLPFC and ERS in medial parietal areas, specifically in the right precuneus and left posterior parietal cortex, as well as in the left temporal lobe, namely, the inferior-posterior temporal cortex (Fig. 5). The findings in peak alpha ERD/ERS values at t_{maxima} of these sources are summarized in Table 2. When the alpha band was divided into alpha1 (8–10 Hz) and alpha2 (10–13 Hz), we observed findings similar to those for the full alpha band with respect to power changes in the DLPFC and midparietal areas. In particular, patients with CIP and nPE differed significantly in alpha1 ERS in parietal areas, including the precuneus and the posterior parietal cortex (peak ERS value: CIP 5.4 ± 4.3%; nPE −6.3 ± 4.4; $t = 6.80$, $P < 0.001$), and in alpha2 ERD in the DLPFC (peak ERD value: CIP −7.8 ± 3.5%; nPE −0.68 ± 4.2%; $t = -4.2$, $P < 0.001$). Peak alpha2 ERD values in the mid-prefrontal cortex (BA 9) nearly reached statistical significance (CIP: −5.8 ± 6.3%; nPE: −0.19 ± 3.3%; $t = -3.12$, $P = 0.004$). Because the epilepsy groups markedly differed in task performance, with patients with CIP providing fewer correct answers than those with nPE (Fig. 3), we tested whether these differences in power changes remained constant during equivalent task performance. For that purpose, we reanalyzed the data after excluding patients with CIP with correct-response accuracy < 90% ($N = 4$). This exploratory analysis showed that patients with CIP and nPE performed equally well ($t(20) = -1.68$, $P = 0.127$). As a result, the statistical Brain Voyager maps showed that alpha ERS source in the precuneus (values at t_{maxima}: CIP 6.2 ± 7.4%; nPE −2.9 ± 5.7%; $t = 2.97$, $P = 0.012$) and posterior parietal cortex (values at t_{maxima}: CIP 4.0 ± 4.9%; nPE −4.0 ± 6.2%; $t = 3.28$, $P = 0.007$) disappeared and no longer differed between patients with CIP and nPE; only alpha source-power changes in the right DLPFC and the left temporal cortex remained significant ($P < 0.001$) (Table 2). No significant power changes in the alpha or any other frequency band emerged after the patients with lower task performance were excluded.

A comparison between patients with schizophrenia and healthy controls revealed significantly different power changes, especially in alpha-oscillatory activity, but also, to a lesser extent, in the theta

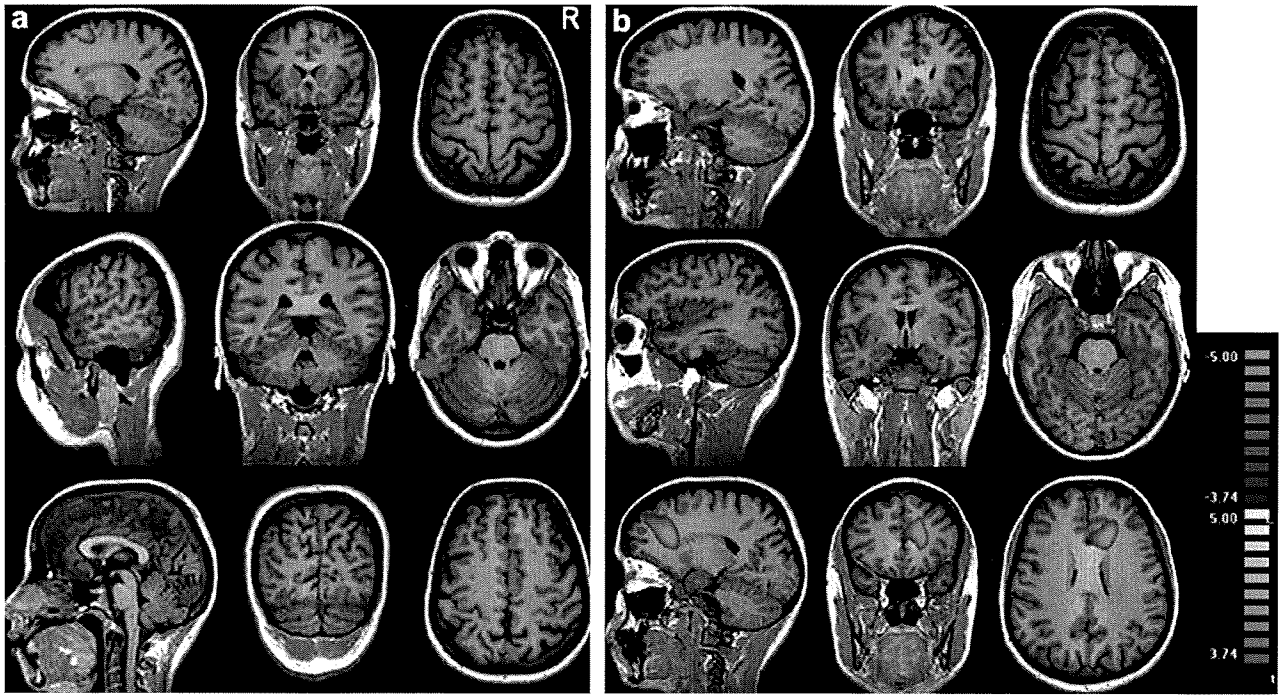

Fig. 5. Statistical maps showing cortical regions with significant between-group differences in power changes in the alpha band during working memory retention in (a) patients with CIP versus patients with nPE and (b) patients with schizophrenia versus healthy controls projected onto a Talairach-transformed T1-weighted anatomical MRI (threshold: $t = 3.74$, $P < 0.001$ uncorrected). The color bars represent the percentages of decrease (blue/green, ERD) and increase (red/yellow, ERS) in oscillatory activity power changes. R, right. (a, bottom panel) The alpha ERS disappeared after exploratory analysis excluding low-performing patients with chronic interictal psychosis. (b, bottom panel) The alpha ERD in the mid-prefrontal cortex was observed in the alpha2 subband only.

Table 2
Cortical regions showing significant between-group differences in oscillatory activity power changes.

ERD/ERS	Location	Talairach (*x*, *y*, *z*)	BA	ERD/ERS at t_{maxima}				*t* value
				CIP	nPE	SCZ	HC	
Alpha ERD	Right SFG	21, 18, 52 19, 20, 52[b]	8	−4.31 ± 2.50	−0.28 ± 2.11	−5.41 ± 3.01	−0.74 ± 2.37	−4.389[c] −4.56[b,c]
				−5.32 ± 1.80	***−5.90***[c]			
Alpha ERS	Right PreC	4, −54, 55	7	6.54 ± 6.13	−2.85 ± 5.70			4.03[c]
				6.15 ± 7.38	***2.97***			
					P = 0.012			
Alpha ERS	Left PPC	−27, −54, 27	7	4.83 ± 4.25	−3.96 ± 6.23			4.254[c]
				3.96 ± 4.93	***3.28***			
					P = 0.007			
Alpha ERS	Left ITG	−57, −29, −12 −37, −10, −23[b]	37 20[b]	0.13 ± 5.19	−9.56 ± 6.72	1.47 ± 6.36	−8.04 ± 6.71	4.14 3.90[b]
				1.16 ± 5.18	***4.18***[c]			
Theta ERS	Left ITG	−41, −8, −24	20			3.15 ± 7.52	−6.17 ± 4.69	3.95[c]
Alpha2 ERD	Right Mid-preF	15, 24, 25	9			−9.16 ± 7.05	2.38 ± 5.16	−4.94[c]

[a]Values in boldface and italic refer to an exploratory analysis excluding low-performing patients with CIP. ERD, event-related desynchronization; ERS, event-related synchronization; BA, Brodmann area; CIP, chronic interictal psychosis; nPE, nonpsychotic epilepsy; SCZ, schizophrenia; HC, healthy controls; SFG, superior frontal gyrus; PreC, precuneus; PPC, posterior parietal cortex; ITG, inferior temporal gyrus; Mid-preF, mid-prefrontal.
[b] Comparison between patients with SCZ and HC.
[c] Significant difference for $P < 0.001$ (uncorrected).

band. The source localization of these activities was similar to those observed in CIP relative to patients with nPE, specifically the right DLPFC and left inferior temporal lobe for alpha activity and the left inferior temporal cortex for the theta band (Fig. 5). The difference in mean values at t_{maxima} of alpha and theta ERD/ERS sources is given in Table 2. Like the full alpha band, the alpha2 subband consistently showed statistically relevant ERD in the right DLPFC (value at t_{maxima}: schizophrenia −9.0 ± 4.2%; healthy controls −0.4 ± 3.2%; $t = -6.04$, $P < 0.001$). However, the alpha2 subband showed an additional ERD source in the right medial prefrontal cortex in patients with schizophrenia.

A comparison between patients with CIP and schizophrenia showed no clear source-power changes in any frequency band, with t_{maxima} in the statistical maps for the alpha band ($t = 3.45$, $P < 0.005$) located over the left inferior parietal cortex, and for the theta band ($t = 2.92$, $P < 0.01$) over the medial-parietal cortex.

3.4. Correlation analysis

To examine the potential influence of medication on source-power changes in patients with CIP and schizophrenia, alpha and theta ERD/ERS mean peak values were correlated with chlorpromazine equivalents and antiepileptic drug (AED) plasma levels. All correlations were two-tailed and controlled for task performance as well as IQ. No statistically significant correlations were identified.

4. Discussion

In the present study, we compared the MEG oscillatory response based on ERD/ERS during a visual-object WM task in patients with CIP, nPE, and schizophrenia and healthy controls to determine whether patients with CIP and primary schizophrenia share WM-related neural abnormalities. Our main findings are: (1) patients with CIP have WM deficits involving a frontotemporal network, (2) the neurophysiological basis for these deficits is primarily changes in the alpha frequency band, and (3) patients with CIP and schizophrenia compare to each other with respect to the WM-compromising brain regions, namely, the right DLPFC and the left temporal cortex, although patients with schizophrenia manifested wider activation in prefrontal areas. In addition, our results showed that the two groups perform at equal levels on a visual-object WM task as far as answer correctness and reaction time are concerned.

4.1. Event-related desynchonization pattern

In this study, frontal lobe WM dysfunction in CIP as well as in schizophrenia manifested as alpha ERD, particularly in the right DLPFC, when compared with patients with nPE and healthy controls (Fig. 5). Given that alpha suppression or desynchronization (i.e., ERD) is considered an electrophysiological correlate of cortical activation involving processing of sensory or cognitive information [30], the prefrontal cortex source-power changes, namely, alpha ERD, seen in our study most likely reflect hyperactivation in both psychotic groups. It is generally accepted that the DLPFC plays a crucial role in WM processing and that its function is impaired in schizophrenia [57]. However, whether its impairment is the result of hyperactivation or hypoactivation is still controversial [58]. Recent analyses have revealed that patients with schizophrenia can show patterns of both hyperactivation and hypoactivation depending on task demands and behavioral performance. Patients with low performance show primarily hypofrontality, whereas high-performing subjects exhibit prefrontal hyperactivation [59]. In this context, it is interesting that the patients with schizophrenia in our study evidenced DLPFC hyperactivation related to WM performance while at the same time performing at par with healthy controls in behavioral accuracy. In addition, high-performing patients with CIP also manifested DLPFC hyperactivation. The fact that the DLPFC activation was detected in the right hemisphere is in line with recent reports proposing that object memory storage is more likely to produce activation in the right prefrontal cortex than storage of other materials (e.g., verbal, visuospatial) [57].

In addition to convergent functional abnormalities in the right DLPFC in the two psychotic groups, we found an alpha2 subband ERD source in the medial prefrontal cortex of patients with schizophrenia, which was not observed when patients with CIP and nPE were compared. This observation is consistent with findings from MRI studies indicating significantly higher medial prefrontal activation [59], particularly in the right side [60] in patients with schizophrenia. As the medial prefrontal cortex is functionally associated with focused attention [35], a function known to be impaired in schizophrenia [16], it is conceivable that the schizophrenic hyperactivation in this area is a reflection of a compensatory mechanism or increased attentional effort in performing

successfully on the WM task. Given that the same pattern of alpha ERD in the medial prefrontal cortex nearly reached statistical significance in CIP when compared with nPE ($P < 0.005$), the possibility that an increase in sample size could also result in significantly different activation in this area for patients with CIP cannot be ruled out.

4.2. Event-related synchronization pattern

The averaged power changes in oscillatory activity in the two psychotic groups revealed that these patients have notable alpha ERS in posterior brain regions, namely, the parieto-occipital and posterior temporal cortex, which was not seen in patients with nPE and healthy subjects (Fig. 4). It is well known that alpha activity typically enhances or synchronizes in the visual (occipital) cortex when subjects are in a relaxed state with their eyes closed, and this phenomenon has therefore been regarded as reflecting mental rest or cortical idling [30]. Thus, alpha ERS in patients with psychosis when engaged in a cognitive task is an intriguing finding. It is important, however, to point out that posterior alpha ERS in eyes-open condition can also occur during motor or cognitive tasks, possibly representing deactivated cortical areas or an inhibited cortical network [61]. In this context, active inhibition in neural networks may be of great importance in optimizing task demands and controlling excitatory processes in cortical areas directly involved in the performance of the task, by blocking, for instance, processing of task-irrelevant sensory or cognitive information [30,36,61]. Nevertheless, the statistical group analysis revealed significant alpha ERS only over the left inferior temporal cortex in the psychotic groups versus their nonpsychotic counterparts (Fig. 5), with the parieto-occipital alpha ERS in patients with CIP being related to poor task performance (Table 2), as discussed below. Interestingly, patients with schizophrenia, and even their nonaffected twins, have been reported to have excessive EEG alpha ERS in cortical areas responsible for processing task-specific visual information during WM retention, correlating in magnitude with memory load [62]. These findings are consistent with the assumption of increased alpha ERS in the posterior-inferior temporal cortex reflecting regional cortical hypoactivation in our study, which most likely indicates WM capacity limitations or inefficiency of cognitive mechanisms subserving active maintenance of information in WM in patients with CIP and schizophrenia [62].

In the schizophrenia group, ERS in the left inferior temporal cortex involved not only the alpha, but also the theta frequency band (Table 2). This finding is in keeping with evidence of alpha and theta oscillations having similar physiological reactivity in WM tasks [32,34]. Similar to our approach, Ince et al. [37] applied MEG and a spectro-temporospatial analysis during the retention phase of a WM task and found that power changes in the theta and alpha bands allowed for successful discrimination between patients with schizophrenia and healthy controls. These authors also noted a left temporal source for the theta ERS, similar to our findings. However, alpha ERS in their study was not distributed over the temporal cortex but over parieto-occipital areas. The discrepancy in the findings may in part be explained by differences in WM storage material, as the aforementioned authors examined verbal WM, whereas our study used a visual nonspatial WM paradigm.

Unlike DLPFC dysfunction, which is largely unexplored in patients with CIP, temporal lobe abnormalities, especially in the left hemisphere, are well linked to both schizophrenia and CIP [10,12,18–25]. Most of the supporting data stem from functional MRI studies in patients with schizophrenia. On the other hand, findings for CIP come from structural MRI, neuropsychological, and neuropathological studies, with very few cognitive functional neuroimaging investigations. Our results of left temporal hypoactivation and a frontotemporal dysfunction during WM in patients with CIP are strengthened by findings from existing functional neuroimaging studies on psychoses in epilepsy, indicating left temporal hypoperfusion using SPECT [23,24] and impaired metabolism in frontal and temporal areas via PET [25]. In addition, correlations between neuropsychological assessments and measures of microstructural integrity in the left temporal lobe as well as in frontotemporal regions in patients with CIP have been reported and provide further support of our findings [19,26]. The ERS sources in patients with CIP and schizophrenia were not visualized in the exact same area within the left inferior temporal cortex, the neural activity in patients with CIP occurring in a more posterior region (Brodmann area 37) compared with that in patients with schizophrenia (Brodmann area 20). However, both areas of the inferior temporal cortex are known to be involved in visual processing of the ventral stream, which is associated with the representation of object features [57]. The finding of left temporal abnormalities in both patients with CIP and those with schizophrenia described herein is thus consistent with dysfunction in cortical regions engaged specifically in performance of the type of task used, namely, visual-object WM.

Alpha ERS in the right precuneus and left posterior parietal cortex clearly distinguished patients with CIP from patients with nPE, yet it was entirely absent in patients with schizophrenia. Interestingly, the ERS in parietal areas was associated with low performance on the task rather than with WM dysfunction itself, as the power changes in oscillatory activity were not significantly different from those of patients with nPE once low-performing patients were excluded (Table 2). Local hypoactivation in the parietal cortex may hence reflect disengagement from the task due to reduced attention in patients with CIP. This would be in agreement with evidence implicating the precuneus and posterior parietal cortex in several modalities of attention such as object-selective attention [63], which is critical to WM, especially for visual object information.

4.3. ERD/ERS sources and external clinical parameters

We tested the potentially confounding effect of medication as most of our patients with psychosis were taking antipsychotic drugs, with the patients with schizophrenia receiving higher doses than the patients with CIP. Patients with CIP were on regular AED treatment. We found no correlation between ERD/ERS sources and chlorpromazine equivalents or AED plasma levels in either psychotic group. This indicates that medication did not influence our findings. The fact that ERD and ERS were calculated as power changes during the memory retention (target) period with respect to the baseline period in the MEG time-series data lends further support to this view, given that medication would equally affect the baseline and the memorization periods. Therefore, normalization with respect to baseline is expected to remove any additive effect.

4.4. Limitations

Some methodological issues in the present study need to be considered. First is sample size. Our CIP sample was relatively small. This is not uncommon in CIP neuroimaging research, and may be the direct result of the difficulty in recruiting patients with CIP and a single brain pathology owing to the relative rarity of the disorder [1,2,6,8]. Nevertheless, we matched patients with CIP for age, gender, type of focal epilepsy, and side of epileptic focus with the nPE group, and patients with low IQ and gross organic lesions were excluded. Second is medication artifacts. Most patients were stably medicated. Based on the results of the correlation analysis of chlorpromazine equivalents and AED plasma levels and the fact that we subtracted time-series data of the baseline period from

those of the memorization (target) period, it is unlikely that pharmacological agents influenced our findings. Third is task dependency. Because we assessed visual-object WM with a fixed memory set of five digits, we cannot rule out that areas engaged in other storage (e.g., verbal or visuospatial) or greater task demands show cortical activation patterns that distinguish CIP from primary schizophrenia if a different paradigm or variation in WM loads is employed. Fourth is diagnostic bias. Patients in the CIP and schizophrenia groups were assessed with different measures of psychotic symptoms, namely, the BPRS for patients with CIP and the PANSS for patients with schizophrenia, which was the result of how the subjects had been ascertained. These two groups can therefore not be directly compared in terms of severity of psychiatric symptoms. Although measures of equivalence between BPRS and PANSS scores in response to antipsychotic treatment were used [64], it is likely that patients with CIP and those with schizophrenia had comparable levels of psychopathology. Regardless, our study was not designed to assess brain activity related to psychopathology itself but to cognitive deficits, in particular WM dysfunction.

4.5. Summary

In this study we found a similar MEG pattern of right DLPFC and left temporal functional abnormalities in patients with CIP and those with schizophrenia during performance of Sternberg's visual WM task, prompting us to consider that similar pathophysiological mechanisms may operate in these two groups. Consistent with this idea, recent studies [13,16] have demonstrated that the profile of neuropsychological impairment in CIP closely resembles that of primary schizophrenia, especially regarding temporal and prefrontal function. Structural MRI of patients with CIP and schizophrenia has further revealed that they share a similar topographic pattern of deficits in temporal and extratemporal cortical gray matter [14]. Together, these data suggest that the DLPFC and temporal cortex are regions closely associated with cognitive dysfunction in both patients with CIP and those with primary schizophrenia, which argues against the concept of CIP as a nosological entity different from schizophrenia. To our knowledge, this is the first neuroimaging study applying MEG for detection of functional cognitive abnormalities in patients with CIP. Larger functional studies on CIP using MEG or different neuroimaging modalities may help elucidate the pathophysiology of chronic psychosis in patients with epilepsy.

Acknowledgments

We thank Christoph Lossin for critical reading of this article, and Dr. Yuka Yasuda, Dr. Hidenaga Yamamori, Dr. Kazutaka Ohi, and Dr. Motoyuki Fukumoto for their contribution in the collection of clinical data of patients with schizophrenia.

References

[1] Sachdev P. Schizophrenia-like psychosis and epilepsy: the status of the association. Am J Psychiatry 1998;155:325–36.
[2] Matsuura M, Trimble MR. Psychoses in epilepsy: a review of Japanese studies. Epilepsy Behav 2000;1:315–26.
[3] Ishii R, Canuet L, Iwase M, et al. Right parietal activation during delusional state in episodic interictal psychosis of epilepsy: a report of two cases. Epilepsy Behav 2006;9:367–72.
[4] Krishnamoorthy ES, Trimble MR, Blumer D. The classification of neuropsychiatric disorders in epilepsy: a proposal by the ILAE Commission on Psychobiology of Epilepsy. Epilepsy Behav 2007;10:349–53.
[5] Slater E, Beard AW, Glithero E. The schizophrenia-like psychoses of epilepsy. Br J Psychiatry 1963;109:95–150.
[6] Cascella NG, Schretlen DJ, Sawa A. Schizophrenia and epilepsy: is there a shared susceptibility? Neurosci Res 2009;63:227–35.
[7] Elliott B, Joyce E, Shorvon S. Delusions, illusions and hallucinations in epilepsy: 2. Complex phenomena and psychosis. Epilepsy Res 2009;85:172–86.
[8] Kanemoto K, Tsuji T, Kawasaki J. Reexamination of interictal psychoses based on DSM IV psychosis classification and international epilepsy classification. Epilepsia 2001;42:98–103.
[9] Adachi N, Matsuura M, Okubo Y, et al. Predictive variables of interictal psychosis in epilepsy. Neurology 2000;55:1310–4.
[10] Perez MM, Trimble MR. Epileptic psychosis: diagnostic comparison with process schizophrenia. Br J Psychiatry 1980;137:245–9.
[11] Toone BK, Garralda ME, Ron MA. The psychoses of epilepsy and the functional psychoses: a clinical and phenomenological comparison. Br J Psychiatry 1982;141:256–61.
[12] Maier M, Mellers J, Toone B, Trimble M, Ron MA. Schizophrenia, temporal lobe epilepsy and psychosis: an in vivo magnetic resonance spectroscopy and imaging study of the hippocampus/amygdala complex. Psychol Med 2000;30:571–81.
[13] Mellers JD, Toone BK, Lishman WA. A neuropsychological comparison of schizophrenia and schizophrenia-like psychosis of epilepsy. Psychol Med 2000;30:325–35.
[14] Marsh L, Sullivan EV, Morrell M, Lim KO, Pfefferbaum A. Structural brain abnormalities in patients with schizophrenia, epilepsy, and epilepsy with chronic interictal psychosis. Psychiatry Res 2001;108:1–15.
[15] Matsuura M, Adachi N, Oana Y, et al. A polydiagnostic and dimensional comparison of epileptic psychoses and schizophrenia spectrum disorders. Schizophr Res 2004;69:189–201.
[16] Nathaniel-James DA, Brown RG, Maier M, Mellers J, Toone B, Ron MA. Cognitive abnormalities in schizophrenia and schizophrenia-like psychosis of epilepsy. J Neuropsychiatry Clin Neurosci 2004;16:472–9.
[17] Tadokoro Y, Oshima T, Kanemoto K. Interictal psychoses in comparison with schizophrenia: a prospective study. Epilepsia 2007;48:2345–51.
[18] Marchetti RL, Azevedo D, de Campos Bottino CM, et al. Volumetric evidence of a left laterality effect in epileptic psychosis. Epilepsy Behav 2003;4:234–40.
[19] Flügel D, Cercignani M, Symms MR, et al. Diffusion tensor imaging findings and their correlation with neuropsychological deficits in patients with temporal lobe epilepsy and interictal psychosis. Epilepsia 2006;47:941–4.
[20] Flügel D, Cercignani M, Symms MR, Koepp MJ, Foong J. A magnetization transfer imaging study in patients with temporal lobe epilepsy and interictal psychosis. Biol Psychiatry 2006;59:560–7.
[21] Tebartz Van Elst L, Baeumer D, Lemieux L, et al. Amygdala pathology in psychosis of epilepsy: a magnetic resonance imaging study in patients with temporal lobe epilepsy. Brain 2002;125:140–9.
[22] Rüsch N, Tebartz van Elst L, Baeumer D, Ebert D, Trimble MR. Absence of cortical gray matter abnormalities in psychosis of epilepsy: a voxel-based MRI study in patients with temporal lobe epilepsy. J Neuropsychiatry Clin Neurosci 2004;16:148–55.
[23] Marshall EJ, Syed GM, Fenwick PB, Lishman WA. A pilot study of schizophrenia-like psychosis in epilepsy using single-photon emission computerised tomography. Br J Psychiatry 1993;163:32–6.
[24] Mellers JD, Adachi N, Takei N, Cluckie A, Toone BK, Lishman WA. SPET study of verbal fluency in schizophrenia and epilepsy. Br J Psychiatry 1998;173:69–74.
[25] Gallhofer B, Trimble MR, Frackowiak R, Gibbs J, Jones T. A study of cerebral blood flow and metabolism in epileptic psychosis using positron emission tomography and oxygen. J Neurol Neurosurg Psychiatry 1985;48:201–6.
[26] Flügel D, O'Toole A, Thompson PJ, et al. A neuropsychological study of patients with temporal lobe epilepsy and chronic interictal psychosis. Epilepsy Res 2006;71:117–28.
[27] Silver H, Feldman P, Bilker W, Gur RC. Working memory deficit as a core neuropsychological dysfunction in schizophrenia. Am J Psychiatry 2003;160:1809–16.
[28] Perlstein WM, Carter CS, Noll DC, Cohen JD. Relation of prefrontal cortex dysfunction to working memory and symptoms in schizophrenia. Am J Psychiatry 2001;158:1105–13.
[29] Uhlhaas PJ, Haenschel C, Nikolić D, Singer W. The role of oscillations and synchrony in cortical networks and their putative relevance for the pathophysiology of schizophrenia. Schizophr Bull 2008;34:927–43.
[30] Pfurtscheller G, Lopes da Silva FH. Event-related EEG/MEG synchronization and desynchronization: basic principles. Clin Neurophysiol 1999;110:1842–57.
[31] Ishii R, Canuet L, Herdman A, et al. Cortical oscillatory power changes during auditory oddball task revealed by spatially filtered magnetoencephalography. Clin Neurophysiol 2009;120:497–504.
[32] Klimesch W. EEG alpha and theta oscillations reflect cognitive and memory performance: a review and analysis. Brain Res Rev 1999;29:169–95.
[33] Jensen O, Tesche CD. Frontal theta activity in humans increases with memory load in a working memory task. Eur J Neurosci 2002;15:1395–9.
[34] Harmony T, Alba A, Marroquín JL, González-Frankenberger B. Time-frequency-topographic analysis of induced power and synchrony of EEG signals during a Go/No-Go task. Int J Psychophysiol 2009;71:9–16.
[35] Ishii R, Shinosaki K, Ukai S, et al. Medial prefrontal cortex generates frontal midline theta rhythm. NeuroReport 1999;10:675–9.
[36] Klimesch W, Sauseng P, Hanslmayr S. EEG alpha oscillations: the inhibition-timing hypothesis. Brain Res Rev 2007;53:63–88.
[37] Ince NF, Goksu F, Pellizzer G, Tewfik A, Stephane M. Selection of spectro-temporal patterns in multichannel MEG with support vector machines for schizophrenia classification. Conf Proc IEEE Eng Med Biol Soc 2008:3554–7.

[38] Ince NF, Pellizzer G, Tewfik AH, et al. Classification of schizophrenia with spectro-temporo-spatial MEG patterns in working memory. Clin Neurophysiol 2009;120:1123–34.
[39] Aine CJ. A conceptual overview and critique of functional neuroimaging techniques in humans: I. MRI/FMRI and PET. Crit Rev Neurobiol 1995;9:229–309.
[40] Ishii R, Shinosaki K, Ikejiri Y, et al. Theta rhythm increases in left superior temporal cortex during auditory hallucinations in schizophrenia: a case report. NeuroReport 2000;11:3283–7.
[41] Canuet L, Ishii R, Iwase M, et al. Factors associated with impaired quality of life in younger and older adults with epilepsy. Epilepsy Res 2009;83: 58–65.
[42] Canuet L, Ishii R, Iwase M, et al. Cephalic auras of supplementary motor area origin: an ictal MEG and SAM(g2) study. Epilepsy Behav 2008;13:570–4.
[43] Ishii R, Canuet L, Ochi A, et al. Spatially filtered magnetoencephalography compared with electrocorticography to identify intrinsically epileptogenic focal cortical dysplasia. Epilepsy Res 2008;81:228–32.
[44] Ohi K, Hashimoto R, Yasuda Y, et al. TATA box-binding protein gene is associated with risk for schizophrenia, age at onset and prefrontal function. Genes Brain Behav 2009;8:473–80.
[45] First MB, Spitzer RL, Gibbon M, Williams JBW. Structured Clinical Interview for DSM-IV Axis I Disorders, Research Version, Non-patients Edition (SCID-I/NP). New York: Biometrics Research, New York State Psychiatric Institute; 2002.
[46] Oldfield RC. The assessment and analysis of handedness: the Edinburgh Inventory. Neuropsychologia 1971;9:97–113.
[47] Mueser KT, Curran PJ, McHugo GJ. Factor structure of the Brief Psychiatric Rating Scale in schizophrenia. Psychol Assess 1997;9:196–204.
[48] Kay SR, Fiszbein A, Opler LA. The Positive and Negative Syndrome Scale (PANSS) for schizophrenia. Schizophr Bull 1987;13:261–76.
[49] Matsuoka K, Uno M, Kasai K, Koyama K, Kim Y. Estimation of premorbid IQ in individuals with Alzheimer's disease using Japanese ideographic script (Kanji) compound words: Japanese version of National Adult Reading Test. Psychiatry Clin Neurosci 2006;60:332–9.
[50] Sternberg S. High-speed scanning in human memory. Science 1966;153: 652–4.
[51] Ihara A, Kakigi R. Oscillatory activity in the occipitotemporal area related to the visual perception of letters of a first/second language and pseudoletters. NeuroImage 2006;29:789–96.
[52] Gross J, Kujala J, Hamalainen M, Timmermann L, Schnitzler A, Salmelin R. Dynamic imaging of coherent sources: studying neural interactions in the human brain. Proc Natl Acad Sci USA 2001;98:694–9.
[53] Hoechstetter K, Bornfleth H, Weckesser D, Ille N, Berg P, Scherg M. BESA source coherence: a new method to study cortical oscillatory coupling. Brain Topogr 2004;16:233–8.
[54] Goebel R, Esposito F, Formisano E. Analysis of functional image analysis contest (FIAC) data with brainvoyager QX: from single-subject to cortically aligned group general linear model analysis and self-organizing group independent component analysis. Hum Brain Mapp 2006;27:392–401.
[55] Kurimoto R, Ishii R, Canuet L, et al. Event-related synchronization of alpha activity in early Alzheimer's disease and mild cognitive impairment: an MEG study combining beamformer and group comparison. Neurosci Lett 2008;443:86–9.
[56] Malhi GS, Lagopoulos J, Das P, Moss K, Berk M, Coulston CM. A functional MRI study of Theory of Mind in euthymic bipolar disorder patients. Bipolar Disord 2008;10:943–56.
[57] Wager TD, Smith EE. Neuroimaging studies of working memory: a meta-analysis. Cogn Affect Behav Neurosci 2003;3:255–74.
[58] Manoach DS. Prefrontal cortex dysfunction during working memory performance in schizophrenia: reconciling discrepant findings. Schizophr Res 2003;60:285–98.
[59] Johnson MR, Morris NA, Astur RS, et al. A functional magnetic resonance imaging study of working memory abnormalities in schizophrenia. Biol Psychiatry 2006;60:11–21.
[60] Thermenos HW, Goldstein JM, Buka SL, et al. The effect of working memory performance on functional MRI in schizophrenia. Schizophr Res 2005;74:179–94.
[61] Neuper C, Pfurtscheller G. Event-related dynamics of cortical rhythms: frequency-specific features and functional correlates. Int J Psychophysiol 2001;43:41–58.
[62] Bachman P, Kim J, Yee CM, et al. Abnormally high EEG alpha synchrony during working memory maintenance in twins discordant for schizophrenia. Schizophr Res 2008;103:293–7.
[63] Shomstein S, Behrmann M. Cortical systems mediating visual attention to both objects and spatial locations. Proc Natl Acad Sci USA 2006;103:11387–92.
[64] Andreasen NC, Carpenter Jr WT, Kane JM, Lasser RA, Marder SR, Weinberger DR. Remission in schizophrenia: proposed criteria and rationale for consensus. Am J Psychiatry 2005;162:441–9.

Dysbindin Regulates the Transcriptional Level of Myristoylated Alanine-Rich Protein Kinase C Substrate *via* the Interaction with NF-YB in Mice Brain

Hiroaki Okuda[1,2☯], Ryusuke Kuwahara[1☯], Shinsuke Matsuzaki[1,3,4☯*], Shingo Miyata[1,3], Natsuko Kumamoto[1], Tsuyoshi Hattori[1,3], Shoko Shimizu[1], Kohei Yamada[1], Keisuke Kawamoto[1], Ryota Hashimoto[3,5], Masatoshi Takeda[5], Taiichi Katayama[4], Masaya Tohyama[1,3,4]

1 Department of Anatomy and Neuroscience, Graduate School of Medicine, Osaka University, Osaka, Japan, **2** Department of Second Anatomy, Faculty of Medicine, Nara Medical University, Nara, Japan, **3** The Osaka-Hamamatsu Joint Research Center for Child Mental Development, Graduate School of Medicine, Osaka University, Osaka, Japan, **4** Department of Child Development and Molecular Brain Science, United Graduate School of Child Development, Osaka University, Kanazawa University and Hamamatsu University School of Medicine, Osaka, Japan, **5** Department of Psychiatry, Osaka University Graduate School of Medicine, Osaka, Japan

Abstract

Background: An accumulating body of evidence suggests that Dtnbp1 (Dysbindin) is a key susceptibility gene for schizophrenia. Using the yeast-two-hybrid screening system, we examined the candidate proteins interacting with Dysbindin and revealed one of these candidates to be the transcription factor NF-YB.

Methods: We employed an immunoprecipitation (IP) assay to demonstrate the Dysbindin-NF-YB interaction. DNA chips were used to screen for altered expression of genes in cells in which Dysbindin or NF-YB was down regulated, while Chromatin IP and Reporter assays were used to confirm the involvement of these genes in transcription of Myristoylated alanine-rich protein kinase C substrate (MARCKS). The sdy mutant mice with a deletion in Dysbindin, which exhibit behavioral abnormalities, and wild-type DBA2J mice were used to investigate MARCKS expression.

Results: We revealed an interaction between Dysbindin and NF-YB. DNA chips showed that MARCKS expression was increased in both Dysbindin knockdown cells and NF-YB knockdown cells, and Chromatin IP revealed interaction of these proteins at the MARCKS promoter region. Reporter assay results suggested functional involvement of the interaction between Dysbindin and NF-YB in MARCKS transcription levels, *via* the CCAAT motif which is a NF-YB binding sequence. MARCKS expression was increased in sdy mutant mice when compared to wild-type mice.

Conclusions: These findings suggest that abnormal expression of MARCKS *via* dysfunction of Dysbindin might cause impairment of neural transmission and abnormal synaptogenesis. Our results should provide new insights into the mechanisms of neuronal development and the pathogenesis of schizophrenia.

Citation: Okuda H, Kuwahara R, Matsuzaki S, Miyata S, Kumamoto N, et al. (2010) Dysbindin Regulates the Transcriptional Level of Myristoylated Alanine-Rich Protein Kinase C Substrate *via* the Interaction with NF-YB in Mice Brain. PLoS ONE 5(1): e8773. doi:10.1371/journal.pone.0008773

Editor: Kenji Hashimoto, Chiba University Center for Forensic Mental Health, Japan

Received November 4, 2009; **Accepted** December 9, 2009; **Published** January 19, 2010

Funding: This work was supported by grants from the Osaka Medical Research Foundation For Incurable Diseases (Shinsuke Matsuzaki) and the Twenty-First Century Center of Excellence (COE) program and the Global COE program (Hiroaki Okuda, Ryusuke Kuwahara, Shinsuke Matsuzaki, Shingo Miyata, Natsuko Kumamoto, Tsuyoshi Hattori, Shoko Shimizu, Kohei Yamada, Taiichi Katayama and Masaya Tohyama). The funders had no role in study design, data collection and analysis, decision to publish, or preparation of the manuscript.

Competing Interests: The authors have declared that no competing interests exist.

* E-mail: s-matsuzaki@anat2.med.osaka-u.ac.jp

☯ These authors contributed equally to this work.

Introduction

Schizophrenia is a common and devastating psychiatric disorder. Lack of patient compliance, due to undesirable side effects and efficacy restricted to positive symptoms, highlights the need to develop novel therapeutics. The etiology of the disease remains unknown, but in recent years a convergence of genetic, pharmacological, and neuroanatomical findings suggest that neural transmission [1–4] and synapse formation [5–11] are involved in schizophrenia. Recent studies suggest that disturbances of Dysbindin (dystrobrevin-binding protein 1; DTNBP1) are involved in this abnormal neural transmission.

The cause of schizophrenia is thought to involve the combined effects of multiple gene components. Genetic linkage and association studies have identified potential susceptibility genes such as Dysbindin [12,13], Neuregulin [14,15], Catechol-*O*-methyltransferase [16–18] and RG4 [19–22]. In particular, it has been reported that chromosome 6p is one of the highest susceptibility regions in linkage studies of schizophrenia [23,24]. Among them, genetic variants in a gene 6p22.3 expressing Dysbindin, which is identified as a protein interacting with dystrobevins [25], have been shown to be strongly associated with schizophrenia [12].

In studies on postmortem brain tissue, decreased levels of Dysbindin protein [26] and mRNA [27] have been shown in

patients with schizophrenia compared with controls. Chronic treatment of mice with antipsychotics did not affect the expression levels of Dysbindin protein and mRNA in their brains [26,28], suggesting that evidence of lower levels of Dysbindin protein and mRNA in the postmortem brains of schizophrenics is not likely to be a simple artifact of antemortem drug treatment. In addition, previous reports have shown that diverse high-risk single nucleotide polymorphisms (SNPs) and haplotypes could influence Dysbindin mRNA expression [27,29]. These data indicate that the Dysbindin gene may confer susceptibility to schizophrenia through reduced Dysbindin expression.

Several lines of evidence suggest that Dysbindin may be associated with brain function. SNPs in *Dysbindin* have been associated with intermediate cognitive phenotypes related to schizophrenia such as IQ and working and episodic memory, and a Dysbindin haplotype has been associated with higher educational attainment [30,31]. In addition, several reports suggest the involvement of Dysbindin in cognitive functions [32–34]. These findings strongly suggest the importance of Dysbindin in brain function. At the cellular level, Dysbindin is located at both pre- and post-synaptic terminals [26,35], and is thought to be involved in postsynaptic density (PSD) function and the trafficking of receptors (NMDA, GABAergic, and nicotinic). Over-expression of Dysbindin increases glutamate release from pyramidal neurons in cell culture, possibly because of its role in vesicular trafficking [36]. Decreases in Dysbindin mRNA and protein levels have been reported in regions previously implicated in schizophrenia: the prefrontal cortex, midbrain, and hippocampus [26,27]. However, the molecular mechanisms of how decreases in Dysbindin expression may contribute to vulnerability to schizophrenia remain unknown.

Thus, we examined the interacting partners of Dysbindin using yeast two-hybrid analysis in order to help elucidate the function of Dysbindin. These interacting-protein data suggest that Dysbindin is involved in such processes as neurotransmission, cell signaling, the cytoskeleton and transcription. (Matsuzaki S *et al.* in submission). In addition, our previous reports suggest the following; (1) decreased expression of Dysbindin might increase dopamine release in the brain resulting in the observed abnormal behavior in sdy mice (Dysbindin KO mice) [37,38], (2) Dysbindin is likely involved in dopaminergic or glutamatergic transmission [36,39], (3) Dysbindin is likely involved in neurotransmission by binding with the BLOC1 complex, and with transcription by binding with transcription-related genes (Matsuzaki S *et al.* in submission), (4) the expression level of Dysbindin may affect the expression of SNAP25 [36,39], (5) Dysbindin may play a key role in coordinating JNK signaling and actin cytoskeleton required for neural development [40]. These findings suggest that Dysbindin may influence neurotransmission and neural development *via* interaction with other factors or by regulation of transcription.

In a previous paper, we identified several Dysbindin interacting partners including the transcription factor, nuclear transcription factor Y beta (NF-YB) (Matsuzaki S *et al.* in submission). NF-YB belongs to a family of CCAAT-binding transcription factors, which are important for the basal transcription of a class of regulatory genes and are involved in cellular reactions [41–44]. Subsequently, in this study, we examined the functional involvement of Dysbindin in transcription *via* its interaction with NF-YB. As a result, we showed that the NF-YB/Dysbindin complex regulates the transcription of MARCKS *via* interaction with certain CCAAT sequences, and abnormal NF-YB/Dysbindin interaction could cause alterations such as impaired neural transmission and abnormal development of neurons.

Results

Dysbindin Exists within the Nucleus in Addition to the Cytoplasm

We examined the existence of Dysbindin in the nucleus, because Dysbindin should exist within the nucleus to play a functional role in transcriptional regulation. We used an overexpression vector for Dysbindin tagged with –FLAG or –V5 to check the intracellular localization of Dysbindin. The fractionation study using Dysbindin-FLAG-overexpressing HEK293 cells shows that Dysbindin exists mainly in the cytosol while a small amount exists in the nucleus (Figure 1A), and Dysbindin-V5 showed the same results (data not shown). These results are in accordance with a previous report [45]. Morphologically, Dysbindin is localized mainly in the cytoplasm with a perinuclear high density region in HEK293 cells and SY5Y cells; however, a faint immunoreaction was also seen within the nucleus (Figure 1B -a and -b). Furthermore, pretreatment with leptomycine-B (LPB), which inhibits export from the nucleus to the cytoplasm, caused a slight Dysbindin increase in cells, which then showed nuclear localization of Dysbindin (Figure 1B -c and -d). These findings suggest that Dysbindin protein is shuttled between the nucleus and the cytoplasm.

Dysbindin Binds to the Transcription Factor NF-YB

Using yeast two-hybrid screening, we identified several transcriptional factors as candidates that may interact with Dysbindin. We selected NF-YB, one of the candidates, and confirmed a Dysbindin-NF-YB interaction by immunoprecipitation assay using HEK293T cells which express NF-YB endogenously (Figure 1A). HEK293T cells were transfected with expression vectors for Dysbindin-V5, and cell lysates were subjected to immunoprecipitation with anti-V5 or anti-NF-YB antibodies, followed by Western blot analysis with a reciprocal antibody. NF-YB was detected in the immunoprecipitates with an anti-V5 body, comparing to the immunoprecipitates with control IgG (Figure 2A), while Dysbindin-V5 was detected in the immunoprecipitates with an anti-NF-YB antibody, comparing to control IgG (data not shown). Thus, Dysbindin and NF-YB are physiologically associated with each other in transfected mammalian cells.

To further our research, we produced a specific anti-Dysbindin antibody with high titer. The antibody detects endogenous Dysbindin in cell and mouse brain samples, though it did not detect any bands corresponding to Dysbindin from the lysates of

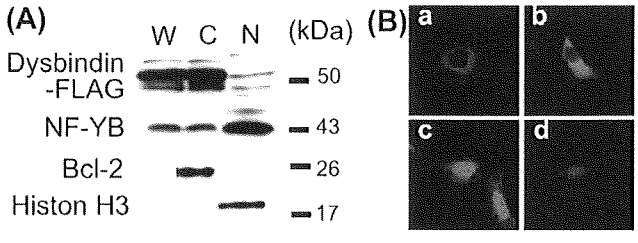

Figure 1. The nuclear localization of Dysbindin. (A) HEK293 cells overexpressing Dysbindin-FLAG were separated into nuclear and cytosolic fractions. Anti-Bcl2 antibody was used for the cytosolic fraction marker and anti-Histone H3 antibody was used for the nuclear fraction marker. W: Whole cell lysates, N: Nuclear Fraction, C: Cytosolic fraction. Dysbindin-FLAG was slightly present in the nuclear fraction. (B) Dysbindin-GFP was overexpressed in HEK293 cells (a and c) or in SH-SY5Y cells (b and d). Dysbindin was usually localized in the cytoplasm and slightly in the nucleus (a and b). After treatment with LMB, a potent inhibitor of CRM1-dependent nuclear export, Dysbindin-GFP accumulated in the nucleus (c and d).
doi:10.1371/journal.pone.0008773.g001

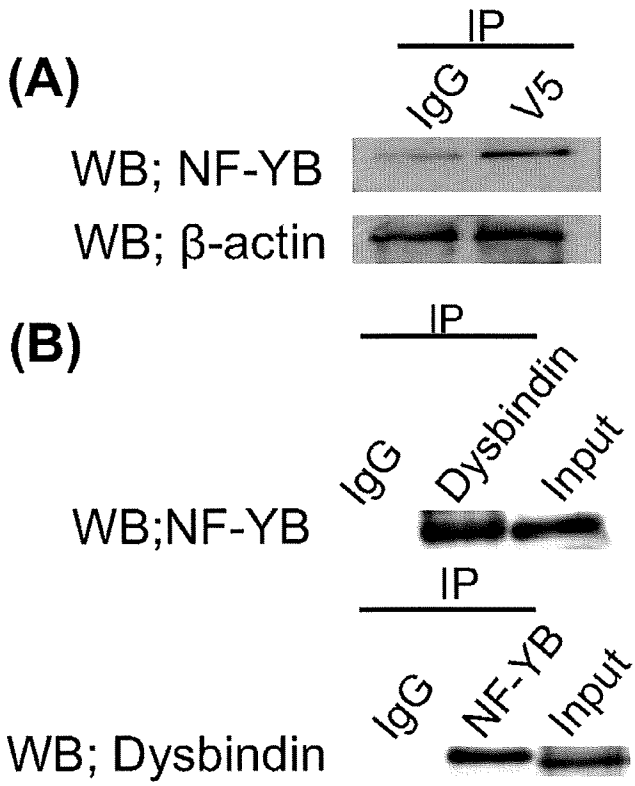

Figure 2. The interaction between Dysbindin and NF-YB. (A) HEK293 cells were transfected with Dysbindin-V5. Immunoprecipitates (IP) of lysates of HEK293 cells expressing Dysbindin-V5 obtained by antibodies to tag proteins (V5) (2nd lane), or nonspecific rabbit IgG (IgG) (1st lane) were subjected to Western blot with anti- NF-YB antibody (upper panel). Dilutions of the lysate (5%, HEK293 cells) were subjected to Western blot with anti-β-actin antibody (lower panel). (**B**) Immunoprecipitates (IP) of lysates of SH-SY5Y cells obtained by antibodies to Dysbindin (upper panel 2nd lane), NF-YB (lower panel 2nd lane), or nonspecific rabbit IgG (IgG) (1st lane of both panels) were subjected to Western blot with anti- NF-YB antibody (upper panel) or Dysbindin antibody (lower panel). Dilutions of the lysate (5%, HEK293 cells) were subjected to Western blot with anti-NF-YB antibody (3rd lane of upper panel) or Dysbindin antibody (3rd lane of lower panel).
doi:10.1371/journal.pone.0008773.g002

Dysbindin knockout mouse brain [40]. The existence of endogenous Dysbindin and endogenous NF-YB in lysates from SH-SY5Y cells was confirmed by Western Blot (Figure 2B, 3rd lane of both panels). Immunoprecipitation using the lysates with antibodies for Dysbindin and NF-YB and subsequent Western blot revealed the interaction of endogenous Dysbindin with endogenous NF-YB (Figure 2B, 2nd lane of both panels), and this binding was also confirmed using adult mouse brain lysates (data not shown).

Downregulation of Dysbindin Causes Upregulation in Expression Levels of Myristoylated Alanine-Rich Protein Kinase C Substrate (MARCKS)

As shown above, we had revealed an interaction between Dysbindin and NF-YB. This result suggests that Dysbindin may be functionally involved in transcription of some genes regulated by NF-YB. We screened for genes displaying altered expression by means of a DNA chip, using RNA extracts from the Dysbindin or NF-YB knockdown human neural cell line, SH-SY5Y. The expression of either *Dysbindin* or *NF-YB* was decreased by the corresponding siRNA for each gene, and the effects of siRNA on Dysbindin or NF-YB were confirmed by Western blot analysis (Figure S1). The genes showing increased expression in the Dysbindin knockdown cells, as well as in the NF-YB knockdown cells, are listed in Table 1A, while those showing decreased expression are listed in Table 1B. Next, using the DANASIS 2.0 system or sequencing of the promoter region, we screened for genes having the CCAAT sequence in the promoter region, because NF-YB is known to bind with high specificity to the CCAAT motif in the promoter region of a variety of genes (Table 1, gene names shown in red). We then focused on three genes; Myristoylated alanine-rich protein kinase C substrate (*MARCKS*) [46–48], Phospholipase C beta 4 (*PLCB4*) [49] and Synaptotagmin 1 (*SYT1*) [50], because an accumulating number of reports point to the involvement of impaired neural transmission in the schizo-

Table 1. The list of genes altered by Dysbindin as well as NF-YB.

(A) Upregulated genes

Dysbindin		NF-YB		
2 h	**24 h**	**2 h**	**24 h**	**Gene name**
1.343	1.393	1.234	1.409	"Chaperonin containing TCP1, subunit 4 (delta)"
1.344	1.325	1.232	1.352	BCL2-associated athanogene
1.296	1.406	1.485	1.394	***Thymine-DNA glycosylase***
1.315	1.476	1.261	1.295	***Myristoylated alanine-rich protein kinase C substrate***
1.355	1.559	1.430	1.434	Homer homolog 3 (Drosophila)
1.411	1.400	1.368	1.224	Hypothetical protein MGC2749
1.238	2.037	1.368	1.259	***Secretogranin II (chromograninC)***

(B) Decreased genes

Dysbindin		NF-YB		
2 h	**24 h**	**2 h**	**24 h**	**Gene name**
0.768	0.701	0.762	0.642	***Brain protein 44-like***
0.747	0.649	0.757	0.677	***Jun dimerization protein 2***
0.827	0.643	0.805	0.803	Kinesin family member 3A
0.734	0.790	0.764	0.601	Sarcosine dehydrogenase
0.814	0.698	0.762	0.722	***Phospholipase C, beta 4"***
0.761	0.645	0.670	0.699	***Synaptotagmin I***
0.815	0.518	0.741	0.780	B cell RAG associated protein
0.729	0.634	0.790	0.796	Hypothetical protein FLJ39370
0.763	0.631	0.760	0.668	SEC63-like (S. cerevisiae)
0.813	0.776	0.824	0.811	***ADP-ribosylation-like factor 6 interacting protein 5***
0.732	0.588	0.608	0.749	***Prothymosin, alpha (gene sequence 28)"***
0.693	0.645	0.769	0.787	***Homeodomain interacting protein kinase 3***
0.710	0.711	0.744	0.618	Similar to AV028368 protein
0.772	0.759	0.762	0.682	***Tropomyosin 4***
0.833	0.651	0.819	0.753	Lactate dehydrogenase A

(A) The genes upregulated by the knockdown of Dysbindin that were in common with those upregulated by the knockdown of NF-YB are listed. The genes showed by bold and italic format have the CCAAT motif.
(B) The genes downregulated by the knockdown of Dysbindin that were in common with those downregulated by the knockdown of NF-YB are listed. The genes showed by bold and italic format have the CCAAT motif.
doi:10.1371/journal.pone.0008773.t001

phrenia pathology. In addition, we considered the involvement of the genes in psychiatric diseases and we narrow down to MARCKS [51] and SYT1 [52]. Interestingly, a previous report suggests the alteration of SYT1 in schizophrenia patients [52]. The paper shows increase of SYT1 mRNA in younger schizophrenia patients group, while it shows decrease of SYT1 mRNA in older schizophrenia patients. These results suggest the complicated and multiple regulation of SYT1 transcriptional regulation. Thus, we examined the functional involvement of the Dysbindin-NF-YB interaction in *MARCKS* transcription.

To confirm the involvement of the knockdown of Dysbindin or NF-YB in the upregulation of MARCKS, we performed Western blot analysis using Dysbindin or NF-YB knockdown SH-SY5Ycells. Comparing the expression level of the MARCKS protein with that of control cells, Dysbindin knockdown cells showed upregulation of MARCKS protein (Figure 3A). To confirm the effect of Dysbindin on MARCKS *in vivo*, we examined the expression of MARCKS protein in the hippocampus with advancing age of the Dysbindin knockout mice, comparing with that found in wild-type mice. In the wild-type mice, a peak in MARCKS protein expression in the hippocampus was identified at postnatal day 15 and 20 (Figure 3B), and then decreased markedly over time. However, such a decrease was not observed in the Dysbindin knockout mice, where large amounts of Dysbindin protein were still expressed in the hippocampii of older mice (Figure 3B). These findings suggest that downregulation of Dysbindin may enhance transcription of the *MARCKS* gene, resulting in the upregulation of MARCKS protein.

We performed chromatin IP analysis using SH-SY5Y cells over-expressing Dysbindin-Flag, to explore the possibility that the Dysbindin-NF-YB complex could affect the transcription of *MARCKS via* interaction with the promoter region of *MARCKS*. The cells were stimulated by retinoic acid to induce *MARCKS*, and were collected as the samples for chromatin IP. PCR products from the chromatin IPs suggest that Dysbindin and NF-YB simultaneously interact with the promoter region of *MARCKS*, but control IgG experiments did not show this result (Figure 3C). These findings indicate that the Dysbindin-NF-YB complex interacts with the promoter region of the *MARCKS* gene resulting in inhibition of *MARCKS* transcription.

The Transcriptional Level of the *MARCKS* Gene Is Regulated by Dysbindin *via* the NF-YB Binding Motif, CCAAT-2

As shown in Figure 4A, the 5′−UTR region of the *MARCKS* gene has two kinds of CCAAT sequences; one CCAAT motif located between UTR −1152 and −700 and the other located between UTR −700 and −614. In this study, we tentatively named the former CCAAT sequence "CCAAT-1" and the latter "CCAAT-2." It is well known that NF-YB binds to the CCAAT motif to regulate transcription of target genes. Thus, we examined whether CCAAT motifs are essential to the regulation of *MARCKS* transcription by means of a luciferase assay, using the following five vectors containing shorter RNA probes; UTR(1152)-Luc, UTR (953)-Luc, UTR(700)-Luc, UTR(614)-Luc, and UTR(462)-Luc (Figure 4A). These constructs were transiently transfected into SH-SY5Y cells which express Dysbindin and NF-YB endogenously, and luciferase activity in each cell line was measured 24 hours after stimulation with retinoic acid. As baseline, we used luciferase activity detected in the SH-SY5Y cells expressing the UTR(1152)-Luc after retinoic acid stimulation (Figure 4A). In the cells transfected with UTR (953)-Luc containing both CCAAT sequences and UTR(700)-Luc containing the CCAAT-1 sequence but lacking the CCAAT-2 sequence, luciferase activity remained at baseline level after stimulation with retinoic acid (Figure 4A). However, luciferase activity was markedly increased in the cells expressing UTR(614)-Luc after retinoic acid stimulation (Figure 4A). These results suggest that the CCAAT-2 motif plays an important role in inhibition of *MARCKS* transcription. Furthermore, the SH-SY5Y cells transfected with UTR(462)-Luc lacking CCAAT-1, CCAAT-2 and the Sp1 region showed very low luciferase activity (Figure 4A), indicating that Sp1 is indispensable for *MARCKS* transcription.

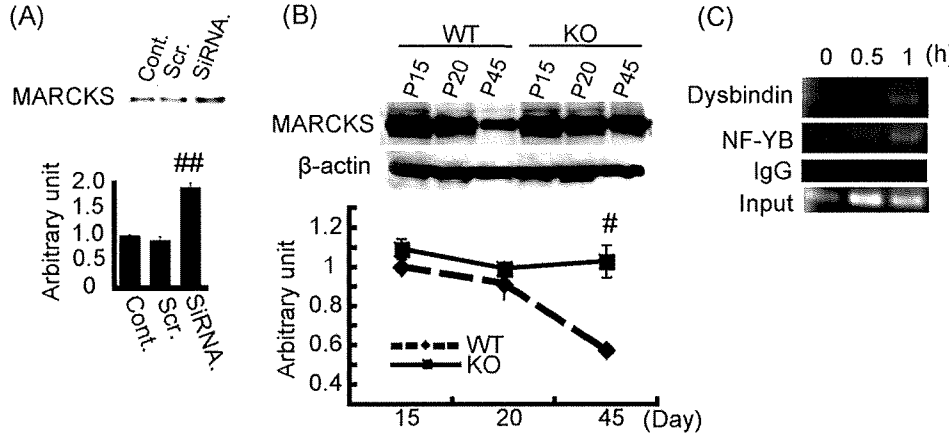

Figure 3. The effects of Dysbindin on MARCKS expression levels. (A) SH-SY5Y cells were transfected with scrambled siRNA or siRNA for Dysbindin. Cell lysate of non-treated cells (Cont.), scrambled RNAi-transfected cells (Scr.) and RNAi for Dysbindin-transfected cells (siRNA) were subjected to Western blot with anti-MARCKS antibody. Columns and vertical bars denote the means ± SEM (triplicate independent experiments). Dysbindin knockdown cells exhibited significant reduction of MARCKS expression compared with control cells ($P<0.001$, Student's t-test). (B) Hippocampus lysates were collected from wild-type mice or Dysbindin KO mice at P15, P20 and P45. The lysates were subjected to Western blot with anti-MARCKS antibody. Graphs and vertical bars denote the means ± SEM (triplicate independent experiments). At P45, Wild-type mice showed significant decreased MARCKS expression, while Dysbindin KO mice showed a maintained MARCKS expression. These data were confirmed by triplicate independent experiments ($P<0.01$, Student's t-test). (**C**)Chromatin IP (ChIP) was performed using SH-SY5Y cells under the stimulation of retinoic acid. The promoter region of *MARCKS* was detected both in the IPs of anti-Dysbindin antibody (1st panel) and those of anti-NF-YB antibody (2nd panel), but not in the IPs of IgG (3rd panel).
doi:10.1371/journal.pone.0008773.g003

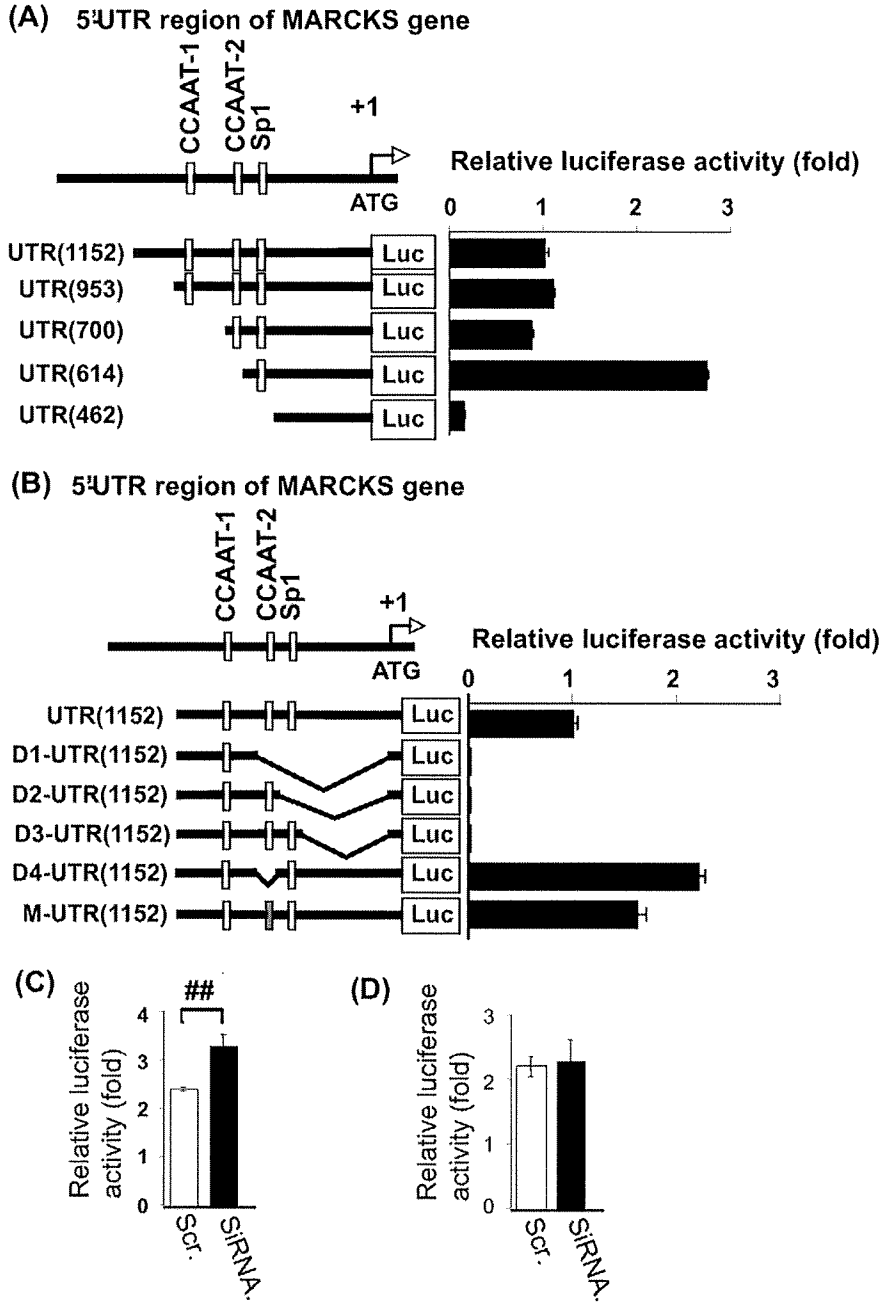

Figure 4. Dysbindin regulates the transcription of MARCKS via the CCAAT2 sequence. (A) The following five vectors were used for luciferase assay, containing shorter DNA probes; UTR(1152)-Luc, UTR (953)-Luc, UTR(700)-Luc, UTR(614)-Luc, and UTR(462)-Luc, were transfected into SH-SY5Y cells and Luciferase activity was measured. UTR(614), which lacks CCAAT1, showed increased luciferase activity. The luciferase activity of UTR(1152) was used as control. Columns and vertical bars denote the means ± SEM (triplicate independent experiments). (B) UTR(1152)-Luc vector and deleted or point mutation of UTR(1152)-Luc vectors, [D1-UTR(1152)-Luc], [D2-UTR(1152)-Luc], [D3-UTR(1152)-Luc] [D4-UTR(1152)-Luc] and [M-UTR(1152)-Luc], were transfected into SH-SY5Y cells and Luciferase activity was measured. [D4-UTR(1152)-Luc], which lacks CCAAT2, and [M-UTR(1152)-Luc], which has a point mutation in the CCAAT2 sequence, showed increased luciferase activity. The luciferase activity of UTR(1152) was used as the control. Columns and vertical bars denote the means ± SEM (triplicate independent experiments). (C and D) Scrambled RNAi-transfected SH-SY5Y cells and Dysbindin RNAi-transfected SH-SY5Y cells were transfected with the UTR(1152)-Luc vector (C) or D4-UTR(1152)-Luc (D) and Luciferase activity was measured. UTR(1152)-Luc vector-expressing cells showed the effect of Dysbindin expression levels on luciferase activity, but D4-UTR(1152)-Luc expressing cells did not. Columns and vertical bars denote the means ± SEM (triplicate independent experiments; $P<0.001$, Student's t-test).
doi:10.1371/journal.pone.0008773.g004

To confirm that the CCAAT-2 region is important in regulation of *MARCKS* transcription, we prepared several probes for the luciferase assay; D1-UTR(1152)-Luc which lacks the CCAAT-2 motif and its downstream region including Sp1 from UTR(1152)-Luc, D2-UTR(1152)-Luc which lacks the Sp1 region and downstream sequence from UTR(1152)-Luc, D3-UTR(1152)-Luc which lacks only sequence downstream of the Sp1 region, D4-UTR(1152)-Luc which lacks only the CCAAT-2 motif from

UTR(1152)-Luc, and M-UTR(1152)-Luc which has a point mutation in the CCAAT-2 motif (Figure 4B). Luciferase activity was detected from the SH-SY5Y cells transfected with each probe, and luciferase activity detected in the cells transfected with UTR(1152)-Luc was used as the baseline value (Figure 4B). Cells transfected with M-UTR(1152)-Luc and those transfected with D4-UTR(1152)-Luc exhibited marked increases in luciferase activity (Figure 4B), showing that the CCAAT-2 motif plays a key role in inhibition of *MARCKS* transcription. Furthermore, cells expressing D1-UTR(1152)-Luc, D2-UTR(1152)-Luc or D3-UTR(1152)-Luc exhibited no luciferase activity. These findings suggest that the sequence downstream of the Sp1 region, as well as the Sp1 region itself, is indispensable for *MARCKS* transcription.

To confirm the involvement of Dysbindin in the altered *MARCKS* transcription levels *via* the CCAAT-2 motif, we compared the luciferase activity of UTR(1152)-Luc detected in Dysbindin knockdown cells with that of control cells. As shown in Figure 4C, knockdown of Dysbindin resulted in upregulation of luciferase activity in the UTR(1152)-Luc transfected cells. However, the effect of knockdown of Dysbindin on luciferase activity was not observed in the D1-UTR(1152)-Luc transfected cells (Figure 4D). These results suggest that Dysbindin regulates *MARCKS* transcription *via* the CCAAT2 motif; the NF-YB binding site. On the other hand, since negligible levels of luciferase activity were observed in cells transfected with any of the probes lacking the sequence downstream of the Sp1 region, the sequence downstream of Sp1 appears to be essential for *MARCKS* transcription (Figure 4A and 4B).

Discussion

Numerous reports support the role of Dysbindin in the etiology of schizophrenia [13,30,37,53–60]. Previous studies have reported a decrease in Dysbindin expression in the brains of schizophrenic patients both at the mRNA and protein levels [26,27]. However, the functional involvement of Dysbindin in the neural system is not yet well elucidated. In this study, we examined involvement of Dysbindin in neural transmission and neural formation *via* transcriptional regulation, because abnormalities in these neural processes are very important in the pathogenesis of schizophrenia.

Regulation of *MARCKS* Transcription by the Dysbindin/NF-YB Interaction

As a result of the yeast-two-hybrid assay and immunoprecipitation assay, we revealed an interaction between NF-YB and Dysbindin (Figure 1 and 2). In addition, we showed the binding of NF-YB and Dysbindin to the *MARCKS* promoter region (Figure 3C). These findings suggest involvement of this complex in transcriptional regulation of MARCKS. As shown in Figure 4, we found two CCAAT sequence motifs at the 5′−UTR of the *MARCKS* gene. Previous reports show that members of the NF-Y family including NF-YB bind to CCAAT sequences and can regulate transcription of a number of genes. Our results suggest that one of the CCAAT sequences, CCAAT-2, is important for *MARCKS* transcriptional regulation. On the other hand, our luciferase assay results suggest that both the Sp1 region and the sequence downstream of Sp1 are indispensable for *MARCKS* transcription (Figure 4A and 4B).

Dysbindin Knockdown Increases MARCKS Protein Levels *In Vivo* and *In Vitro*

In accordance with the enhanced *MARCKS* transcription mediated by the knockdown of Dysbindin, Dysbindin knockdown cells show increased MARCKS levels (Figure 3A). Next, we examined the expression level of MARCKS in Dysbindin knockout mice. As shown in Figure 3b, in the wild-type mouse brain the peak in MARCKS expression is at postnatal day 15; thereafter decreasing markedly with advancing age until only low levels of MARCKS expression are seen in adults (P45). Comparable alternations in MARCKS expression were also observed in another mouse line, ICR (data not shown). These findings support the hypothesis that MARCKS plays an important role in brain development. However, in the Dysbindin knockout mice, there is no effect on MARCKS expression during the developmental stage, when MARCKS is abundantly expressed in wild-type mice. During this stage, *MARCKS* transcription may be regulated by multiple molecules, which compensate for the lack of Dysbindin. With increasing age of the mouse, MARCKS expression decreases gradually to a low level of expression in adults (Figure 3b). In contrast, a decrease in MARCKS expression was not observed in Dysbindin knockout mice (Figure 3b) and even in adult mice brains, a high level of expression of MARCKS was detected. These findings show that Dysbindin likely plays a major role in regulation of MARCKS expression in the adult brain, in contrast to in the developmental stage. Therefore, considering the results in Dysbindin knockout mice, it is likely that MARCKS is expressed at high levels in schizophrenic brains, compared with age-matched control brains.

MARCKS and Neural Transmission

It has been shown that MARCKS impacts on neurotransmission *via* F-actin and on vesicular transport *via* synaptic vesicles [46–48]. Furthermore, many reports indicate that dopaminergic transmission is increased in the brains of schizophrenics [1–4]. Dopamine D2 antagonists are an effective treatment in schizophrenia, and dopamine-enhancing drugs mimic psychotic symptoms of schizophrenia. In the schizophrenic brain, the expression of Dysbindin is decreased, resulting in an increase in MARCKS protein expression, which impacts on neurotransmission. Furthermore, we found that decreases in Dysbindin levels upregulate dopamine release [39]. Therefore, the enhanced dopaminergic transmission produced by the lower expression level of Dysbindin may be partially attributable to activation of MARCKS. Thus, the impairment of neural transmission in the schizophrenic brain may be caused by alterations of MARCKS expression levels *via* changes in Dysbindin.

Dysbindin May Regulate Neural Formation *via* Alteration of MARCKS Levels

Many studies support the hypothesis that schizophrenia is a neurodevelopmental disease. Disrupted-In Schizophrenia 1 (DISC1) is a gene disrupted by a (1;1) (q42.1; q14.3) translocation that segregates with major psychiatric disorders, including schizophrenia in a Scottish family [61,62]. Previously, we examined the physiological role of the molecular complex composed of DISC1 and its interacting partners, Fasciculation and elongation protein zeta 1 (Fez1) [63] and DISC1-Binding Zinc finger protein (DBZ)[64]. Both the DISC1-Fez1 interaction and the DISC1-DBZ interaction are involved in neurite extension. These reports suggest that abnormalities in the schizophrenia susceptibility genes, such as DISC1, likely cause an impairment of brain development resulting in schizophrenia. In addition, several reports suggest that the PKC signal is involved in psychiatric disorders, as well as other signals such as ERK, which play important roles in neural development. In addition, we previously showed the importance of Dysbindin for growth cone formation [40]. These previous reports suggest that abnormal neural formation could cause psychiatric disorders and that Dysbindin

may be one of the important factors in normal neural development. In this study, we demonstrate the transcriptional regulation of MARCKS *via* Dysbindin and the upregulation of MARCKS by downregulation of Dysbindin. Since MARCKS is involved not only in neural transmission[48] but also in neural developmental processes such as synaptogenesis and maintaining spine morphology [46,47], these results suggest that dysfunction of Dysbindin likely causes the upregulation of MARCKS and may induce abnormal development of the nervous system *via* alterations of MARCKS levels.

Thus, in this paper, we report the following findings; (1) Dysbindin interacts with NF-YB, (2) NF-YB and Dysbindin bind to the promoter region of MARCKS, (3) one of the CCAAT sequences is likely essential for the transcriptional regulation of MARCKS and (4) the downregulation of Dysbindin upregulates the expression of MARCKS *in vitro* and *in vivo*. On the other hand, we previously showed that Dysbindin knockout mice exhibit schizophrenia-like behavior and abnormalities of the dopaminergic system. These phenotypes may be at least partly attributable to over-activation of MARCKS *via* a decrease in Dysbindin levels.

In conclusion, these results may help shed some light on the causes of schizophrenia, and indicate that the transcriptional regulation of Dysbindin may contribute to schizophrenia. Further studies of Dysbindin and its association with MARCKS and with schizophrenia may reveal novel treatment targets for schizophrenia.

Materials and Methods

Antibodies

Monoclonal anti-Dysbindin antibody was produced. Briefly, GST-fused human Dysbindin was used as antigen and the Dysbindin protein for ELISA was made by thrombin digestion of GST-Dysbindin. High-titer clones for Dysbindin were selected by ELISA using the Dysbindin protein and the immunoreactivity of the clones was checked by Western blot. Antibodies of anti-GFP (Santa Cruz Biotechnology, Santa Cruz, CA), anti-Flag (Sigma-Aldrich, St Louis, MO), anti-V5 (Invitrogen), anti-β-actin (Chemicon International, Temecula, CA), anti-NF-YB (Santa Cruz Biotechnology), anti-MARCKS (Upstate), HRP-conjugated anti-mouse and Rabbit IgG (Cell Signaling Technology, Beverly, MA), and mouse normal IgG (Sigma-Aldrich) were purchased commercially.

Plasmids

We previously constructed the pEGFP-C1 expression vector (Clontech) carrying the full-length human *Dysbindin* cDNA (-GFP is tagged to N-terminal) [22]. The human Dysbindin-V5 (-V5 is tagged to C-terminal), Dysbindin-FLAG (-FLAG is tagged to N-terminal) and NF-YB moieties were amplified from a human brain cDNA library using PCR and subcloned into pcDNA3.1 (+) expression vector (Invitrogen, Carlsbad, CA). Dysbindin and NF-YB were amplified using rTaq DNA polymerase (Takara Bio Inc., Kyoto, Japan) with the following primer set: Dysbindin-V5, 5′−CTCGAGTTACGTAGAATCGAGACCGAGGAGAGGG-TTAGGGATAGGCTTACCAGAGTCGCTGTCCTCACC−3′-(forward) and 5′−GGTACCGCCACCATGCTGGAGACCCT-TCGCGA−3′ (reverse); NF-YB, 5′−GCTAGCGCCACCAT-GACAATGGATGGTGACAGTTCT−3′ (forward) and 5′−G-ATATCTGAAAACTGAATTTGCTGAAC−3′ (reverse). The amplified fragments were TA cloned into the pGEM-T vector (Promega Corp.).

pMARCKS-Luc(−1152) was generated by subcloning promoters into pGL3-(R2.2) Basic (Promega). We generated 5′ deletion constructs of pMARCKS-Luc(−1152) and an internal deletion construct of the region −700∼−1. Other deletion constructs of the region (−231∼−150) and point mutation constructs of pMARCKS-Luc/dl(−204∼−187), were generated by inserting double-stranded oligonucleotides (Figure 2B and 2D). The plasmid pMARCKS-Luc(−736/mt) was generated by site-directed mutagenesis, which changed the same nucleotides as those of mutant 5.

Cell Culture

Human neuroblastoma SH-SY5Y cells were obtained from the Human Science Research Resources Bank (HSRRB). These cells were maintained in tissue culture dishes (Nalge Nunc, Rochester, NY, USA) in 50% minimal essential medium (Invitrogen) /50% F-12 (Invitrogen) containing 15% heat-inactivated fetal bovine serum (Invitrogen) at 37°C in an atmosphere of 95% air /5% CO_2.

Animals

sdy mice (Dysbindin KO mice) and wild-type littermates were provided by the Takeda lab, Department of Psychiatry, Osaka University Graduate School of Medicine. The mice were deeply anesthetized with sodium pentobarbital. Brains (hippocampus) were dissected from each aged mouse. All animal experiments were carried out in accordance with a protocol approved by the Institutional Animal Care and Use Committee of Osaka University.

Immunocytochemistry

SY5Y cells were grown on poly-l-lysine-coated four-well chamber dishes at a density of 3×10^4 cells/cm^2. The cells were fixed in 2% paraformaldehyde in 0.1 M PBS, permeabilized, and blocked with 0.02 M PBS containing 0.3% Triton X-100, 3% BSA and 10% goat serum for 30 min at room temperature, and then incubated with antibodies specific for the individual protein. Confocal microscopy was performed using a Carl Zeiss LSM-510 confocal microscope.

Fractionation Assay

Cells were collected after washing with ice-cold PBS. Cells and brains were homogenized in Tris buffer (20 mM Tris–HCl, pH 7.8, 1 mM EDTA, 150 mM NaCl and protease inhibitor cocktail (Roche)). After homogenization, the homogenized proteins were lysed by the addition of 0.5% NP-40 for 30 min on ice and centrifuged at 500 ×*g* for 10 min to collect the nuclear pellet. The supernatant was collected as the cytosolic fraction.

Immunoprecipitation (IP)

After washing cells with ice-cold PBS, cells were collected and resuspended in 1 mL lysis buffer (20 mM Tris–HCl, pH 7.8, 0.2% NP-40, 1 mM EDTA, 150 mM NaCl and protease inhibitor cocktail (Roche)). Cells were frozen in dry ice/EtOH and stored at −80°C. Cell lysates were incubated on ice for 30 min and then centrifuged for 5 min at 13,600×*g*. After centrifugation, the supernatants were precleared with protein Sepharose G beads and IP was carried out in lysis buffer with antibody/protein G Sepharose beads for 1 h at 4°C. After washing in lysis buffer, immunoprecipitated proteins were immunoblotted.

Immunoblotting

Aliquots of whole cell lysates or IP lysates separated by SDS-PAGE were blotted onto an Immobilon-P membrane (Millipore), and then incubated with antibodies specific for individual protein. Proteins were detected by ECL plus Western Blotting Detection

System (GE Healthcare), followed by exposure to X-ray films according to the manufacturer's protocol.

Knockdown Experiment Using Small Interfering RNA (siRNA)

Stealth siRNA against Dysbindin (5′−CCAAAGUACUCUGCUGGAUUAGAAU−3′ and 5′−GCUCCCAGCUUUAAUCGCAGACUUA−3′), NF-YB 5′−UACUGAGGACAGCAUGAAUGAUCAU−3′ , and negative control duplexes (scrambled siRNA for Dysbindin, 5′−CCATGATCTCGTCGTTAGAAAGAAA−3′ and 5′−GCTACCGTTATTAGCACAGCCCTTA−3′ ; and scrambled siRNA for NF-YB, 5′−UACGGAACAACGAGUGUAUAUGCAU−3′) were provided by Invitrogen Corp. SY5Y cells were transfected with 100 pM of each siRNA and scrambled siRNA using Lipofectamine 2000 (Invitrogen Corp.) according to the manufacturer's instructions.

RNA Extracts and Microarray

Total RNA was extracted from cells using RNeasy columns (Qiagen) according to the manufacturer's instructions. Five hundred nanograms of total RNA from control and experimental cells was separately amplified and labeled with either Cy3- or Cy5-labeled CTP (Perkin Elmer) with an Agilent low input linear amplification kit (Agilent Technologies) according to manufacturer's instructions. After labeling and cleanup, amplified RNA was quantified by UV-vis spectroscopy. One microgram each of Cy3- and Cy5-labeled targets were combined and hybridized with a Whole Human Genome Oligo Microarray Kit (G4112F)according to the manufacturer's instructions. Three biological replicates were used at each time point with one of the replicates being a dye reversal of the other two. Microarrays were imaged on a Hitachi image scanner and data analyzed with GeneSpring 6 (Silicon Genetics).

Chromatin Immunoprecipitation (ChIP) Assay

ChIP analysis was performed using a Chromatin Immunoprecipitation Assay Kit (Upstate Biotechnology) according to the manufacturer's instructions. Briefly, protein−DNA complexes were crosslinked with 1% formaldehyde (10 min at room temperature) and cells were harvested. DNA was sonicated to lengths of 500−1000 bp. Antibodies specific for individual protein were used for immunoprecipitating protein-DNA complexes overnight at 4°C. PCR was performed with individual specific primer sets for the MARCKS promoter: the proximal CCAAT region, 5′−GGTTTGCTCTTTGATGCTCTTGAT−3′ and 5′−ACTTTCGGGTGGGGTGTAA−3′

Reporter Assay

Reporter plasmids were transfected into cells using Lipofectamine 2000 (Invitrogen) together with phRG-TK (Renilla reporter for internal control) which monitored transfection efficiency. Luciferase activities were assayed using the Dual Luciferase Assay System (Promega). All assays were performed three times in duplicate and values are shown as means ± SD.

Supporting Information

Figure S1 The preparation of mRNAs for microarray analysis. (A-(a) and B-(a)) To prepare RNAs for microarrays analysis, we transfected the siRNA for Dysbindin, NF-YB, or scrambled as a control. The effect of each RNAi was confirmed by Western blot using the antibody for Dysbindin or NF-YB. (A-(b) and B-(b)) The columns and vertical bars denote the means ± SEM (triplicate independent experiments; $P<0.001$, Student's t-test). Dysbindin or NF-YB was knocked-down significantly by transfection of the siRNA for Dysbindin or NF-YB, compared with the control.
Found at: doi:10.1371/journal.pone.0008773.s001 (1.10 MB EPS)

Acknowledgments

We thank Ms. Arakawa, Ms. Moriya, and Ms. Ohashi for preparing our experiments.

Author Contributions

Conceived and designed the experiments: HO SM SM MT. Performed the experiments: HO RK SM. Analyzed the data: HO RK SM SM NK TH RH TK MT. Contributed reagents/materials/analysis tools: SM NK SS KY KK RH MT TK. Wrote the paper: HO RK SM MT.

References

1. Garver DL (2006) Evolution of antipsychotic intervention in the schizophrenic psychosis. Curr Drug Targets 7(9): 1205–1215.
2. Lewis DA, Gonzalez-Burgos G (2006) Pathophysiologically based treatment interventions in schizophrenia. Nat Med 12(9): 1016–1022.
3. Ross CA, Margolis RL, Reading SA, Pletnikov M, Coyle JT (2006) Neurobiology of schizophrenia. Neuron 52(1): 139–153.
4. Mouri A, Noda Y, Enomoto T, Nabeshima T (2007) Phencyclidine animal models of schizophrenia: approaches from abnormality of glutamatergic neurotransmission and neurodevelopment. Neurochem Int 51(2–4): 173–184.
5. CATIE (Clinical Antipsychotic Trials of Intervention Effectiveness) investigators (2005) Effectiveness of antipsychotic drugs in patients with chronic schizophrenia. N Engl J Med 353: 1209–1223.
6. Coyle JT (2006) Glutamate and schizophrenia: Beyond the dopamine hypothesis. Cell Mol Neurobiol 26(4–6): 365–384.
7. Lau CG, Zukin RS (2007) NMDA receptor trafficking in synaptic plasticity and neuropsychiatric disorders. Nat Rev Neurosci 8(6): 413–26.
8. Li B, Woo RS, Mei L, Malinow R (2007) The neuregulin-1 receptor erbB4 controls glutamatergic synapse maturation and plasticity. Neuron 54(4): 583–97.
9. Moghaddam B (2003) Bringing order to the glutamate chaos in schizophrenia. Neuron 40: 881–884.
10. Snyder SH (2006) Dopamine receptor excess and mouse madness. Neuron 49: 484–485.
11. Stephan KE, Baldeweg T, Friston KJ (2006) Synaptic plasticity and dysconnection in schizophrenia. Biol Psychiatry 59(10): 929–39.
12. Straub RE, Jiang Y, MacLean CJ, Ma Y, Webb BT, et al. (2002) Genetic variation in the 6p22.3 gene DTNBP1, the human ortholog of the mouse dysbindin gene, is associated with schizophrenia. Am J Hum Genet 71: 337–348.
13. Schwab SG, Knapp M, Mondabon S, Hallmayer J, Borrmann-Hassenbach M, et al. (2003) Support for association of schizophrenia with genetic variation in the 6p22.3 gene, dysbindin, in sib-pair families with linkage and in an additional sample of triad families. Am J Hum Genet 72: 185–190.
14. Stefansson H, Sigurdsson E, Steinthorsdottir V, Bjornsdottir S, Sigmundsson T, et al. (2002) Neuregulin 1 and susceptibility to schizophrenia. Am J Hum Genet 71: 877–892.
15. Stefansson H, Sarginson J, Kong A, Yates P, Steinthorsdottir V, et al. (2003) Association of neuregulin 1 with schizophrenia confirmed in a Scottish population. Am J Hum Genet 72: 83–87.
16. Egan MF, Goldberg TE, Kolachana BS, Callicott JH, Mazzanti CM, et al. (2001) Effect of COMT Val108/158 Met genotype on frontal lobe function and risk for schizophrenia. Proc Natl Acad Sci U S A 98: 6917–6922.
17. Bilder RM, Volavka J, Czobor P, Malhotra AK, Kennedy JL, et al. (2002) Neurocognitive correlates of the COMT Val(158)Met polymorphism in chronic schizophrenia. Biol Psychiatry 52: 701–707.
18. Shifman S, Bronstein M, Sternfeld M, Pisante-Shalom A, Lev-Lehman E, et al. (2002) A highly significant association between a COMT haplotype and schizophrenia. Am J Hum Genet 71: 1296–1302.
19. Chowdari KV, Mirnics K, Semwal P, Wood J, Lawrence E, et al. (2002) Association and linkage analyses of RGS4 polymorphisms in schizophrenia. Hum Mol Genet 11: 1373–1380.
20. Williams NM, Preece A, Spurlock G, Norton N, Williams HJ, et al. (2004) Support for RGS4 as a susceptibility gene for schizophrenia. Biol Psychiatry 55: 192–195.
21. Chen X, Dunham C, Kendler S, Wang X, O'Neill FA, et al. (2004) Regulator of G-protein signaling 4 (RGS4) gene is associated with schizophrenia in Irish high density families. Am J Med Genet B Neuropsychiatr Genet 129: 23–26.
22. Morris DW, Rodgers A, McGhee KA, Schwaiger S, Scully P, et al. (2004) Confirming RGS4 as a susceptibility gene for schizophrenia. Am J Med Genet B Neuropsychiatr Genet 125: 50–53.

23. Wang S, Sun CE, Walczak CA, Ziegle JS, Kipps BR, et al. (1995) Evidence for a susceptibility locus for schizophrenia on chromosome 6pter-p22. Nat Genet 10: 41–46.
24. Straub RE, MacLean CJ, O'Neill FA, Burke J, Murphy B, et al. (1995) A potential vulnerability locus for schizophrenia on chromosome 6p24-22: evidence for genetic heterogeneity. Nat Genet 11: 287–293.
25. Benson MA, Newey SE, Martin-Rendon E, Hawkes R, Blake DJ (2001) Dysbindin, a novel coiled-coil-containing protein that interacts with the dystrobrevins in muscle and brain. J Biol Chem 276: 24232–24241.
26. Talbot K, Eidem WL, Tinsley CL, Benson MA, Thompson EW, et al. (2004) Dysbindin-1 is reduced in intrinsic, glutamatergic terminals of the hippocampal formation in schizophrenia. J Clin Invest 113(9): 1353–1363.
27. Weickert CS, Straub RE, McClintock BW, Matsumoto M, Hashimoto R, et al. (2004) Human dysbindin (DTNBP1) gene expression in normal brain and in schizophrenic prefrontal cortex and midbrain. Arch Gen Psychiatry 61(6): 544–55.
28. Chiba S, Hashimoto R, Hattori S, Yohda M, Lipska B, et al. (2006) Effect of antipsychotic drugs on DISC1 and dysbindin expression in mouse frontal cortex and hippocampus. J Neural Transm 113(9): 1337–46.
29. Bray NJ, Preece A, Williams NM, Moskvina V, Buckland PR, et al. (2005) Haplotypes at the dystrobrevin binding protein 1 (DTNBP1) gene locus mediate risk for schizophrenia through reduced DTNBP1 expression. Hum Mol Genet 14: 1947–1954.
30. Corvin A, Donohoe G, Nangle JM, Schwaiger S, Morris D, et al. (2008) A dysbindin risk haplotype associated with less severe manic-type symptoms in psychosis. Neurosci Lett 431(2): 146–149.
31. Donohoe G, Morris DW, Clarke S, McGhee KA, Schwaiger S, et al. (2007) Variance in neurocognitive performance is associated with dysbindin-1 in schizophrenia: a preliminary study. Neuropsychologia 45(2): 454–458.
32. Burdick KE, Lencz T, Funke B, Finn CT, Szeszko PR, et al. (2006) Genetic variation in DTNBP1 influences general cognitive ability. Hum Mol Genet 15(10): 1563–8.
33. Luciano M, Miyajima F, Lind PA, Bates TC, Horan M, et al. (2008) Variation in the dysbindin gene and normal cognitive function in three independent population samples. Genes Brain Behav.
34. Zinkstok JR, de Wilde O, van Amelsvoort TA, Tanck MW, Baas F, et al. (2007) Association between the DTNBP1 gene and intelligence: a case-control study in young patients with schizophrenia and related disorders and unaffected siblings. Behav Brain Funct 3: 19.
35. Sillitoe RV, Benson MA, Blake DJ, Hawkes R (2003) Abnormal dysbindin expression in cerebellar mossy fiber synapses in the mdx mouse model of Duchenne muscular dystrophy. J Neurosci 23(16): 6576–85.
36. Numakawa T, Yagasaki Y, Ishimoto T, Okada T, Suzuki T, et al. (2004) Evidence of novel neuronal functions of dysbindin, a susceptibility gene for schizophrenia. Hum Mol Genet 13: 2699–2708.
37. Murotani T, Ishizuka T, Hattori S, Hashimoto R, Matsuzaki S, et al. (2007) High dopamine turnover in the brains of Sandy mice. Neurosci Lett 421(1): 47–51.
38. Hattori S, Murotani T, Matsuzaki S, Ishizuka T, Kumamoto N, et al. (2008) Behavioral abnormalities and dopamine reductions in sdy mutant mice with a deletion in Dtnbp1, a susceptibility gene for schizophrenia. Biochem Biophys Res Commun 373(2): 298–302.
39. Kumamoto N, Matsuzaki S, Inoue K, Hattori T, Shimizu S, et al. (2006) Hyperactivation of Midbrain Dopaminergic System in Schizophrenia could be attributed to the Down-regulation of Dysbindin. Biochem Biophys Res Commun 345(2): 904–905.
40. Kubota K, Kumamoto N, Matsuzaki S, Hashimoto R, Hattori T, et al. (2009) Dysbindin engages in c-Jun N-terminal kinase activity and cytoskeletal organization. Biochem Biophys Res Commun 379: 191–195.
41. Donati G, Imbriano C, Mantovani R (2006) Dynamic recruitment of transcription factors and epigenetic changes on the ER stress response gene promoters. Nucleic Acids Res 34(10): 3116–27.
42. Gurtner A, Manni I, Fuschi P, Mantovani R, Guadagni F, et al. (2003) Requirement for down-regulation of the CCAAT-binding activity of the NF-Y transcription factor during skeletal muscle differentiation. Mol Biol Cell 14(7): 2706–15.
43. Li Q, Herrler M, Landsberger N, Kaludov N, Ogryzko VV, et al. (1998) Xenopus NF-Y pre-sets chromatin to potentiate p300 and acetylation-responsive transcription from the Xenopus hsp70 promoter in vivo. EMBO J 17(21): 6300–15.
44. Maity SN, de Crombrugghe B (1998) Role of the CCAAT-binding protein CBF/NF-Y in transcription. Trends Biochem Sci 23(5): 174–8.
45. Nian H, Fan C, Liao S, Shi Y, Zhang K, et al. (2007) RNF151, a testis-specific RING finger protein, interacts with dysbindin. Arch Biochem Biophys 465(1): 157–163.
46. Trifaró J, Rosé SD, Lejen T, Elzagallaai A (2000) Two pathways control chromaffin cell cortical F-actin dynamics during exocytosis. Biochimie 82(4): 339–352.
47. Sasaki Y (2003) New aspects of neurotransmitter release and exocytosis: Rho-kinase-dependent myristoylated alanine-rich C-kinase substrate phosphorylation and regulation of neurofilament structure in neuronal cells. J Pharmacol Sci 93(1): 35–40.
48. Park YS, Hur EM, Choi BH, Kwak E, Jun DJ, et al. (2006) Involvement of protein kinase C-epsilon in activity-dependent potentiation of large dense-core vesicle exocytosis in chromaffin cells. J Neurosci 26(35): 8999–9005.
49. Maejima T, Oka S, Hashimotodani Y, Ohno-Shosaku T, Aiba A, et al. (2005) Synaptically driven endocannabinoid release requires Ca2+-assisted metabotropic glutamate receptor subtype 1 to phospholipase Cbeta4 signaling cascade in the cerebellum. J Neurosci 25(29): 6826–35.
50. Koh TW, Bellen HJ (2003) Synaptotagmin I, a Ca2+ sensor for neurotransmitter release. Trends Neurosci 26(8): 413–22.
51. Manji HK, Lenox RH (1999) Protein kinase C signaling in the brain: molecular transduction of mood stabilization in the treatment of manic-depressive illness. Biol Psychiatry 46(10): 1328–51.
52. Sokolov BP, Teherepanov AA, Haroutunian V, Davis KL (2000) Levels of mRNAs encoding synaptic vesicle and synaptic plasma membrane proteins in the temporal cortex of elderly schizophrenic patients. Biol Psychiatry 48(3): 184–96.
53. van den Bogaert A, Schumacher J, Schulze TG, Otte AC, Ohlraun S, et al. (2003) The DTNBP1 (dysbindin) gene contributes to schizophrenia, depending on family history of the disease. Am J Hum Genet 73: 1438–1443.
54. Tang JX, Zhou J, Fan JB, Li XW, Shi YY, et al. (2003) Family-based association study of DTNBP1 in 6p22.3 and schizophrenia. Mol Psychiatry 8: 717–718.
55. van den Oord EJ, Sullivan PF, Jiang Y, Walsh D, O'Neill FA, et al. (2003) Identification of a high-risk haplotype for the dystrobrevin binding protein 1(DTNBP1) gene in the Irish study of high-density schizophrenia families. Mol Psychiatry 8: 499–510.
56. Williams NM, Preece A, Morris DW, Spurlock G, Bray NJ, et al. (2004) Identification in 2 independent samples of a novel schizophrenia risk haplotype of the dystrobrevin binding protein gene (DTNBP1). Arch Gen Psychiat 61: 336–344.
57. Funke B, Finn CT, Plocik AM, Lake S, DeRosse P, et al. (2004) Association of the DTNBP1 locus with schizophrenia in a U.S. population. Am J Hum Genet 75: 891–898.
58. Kirov G, Ivanov D, Williams NM, Preece A, Nikolov I, et al. (2004) Strong evidence for association between the dystrobrevin binding protein 1 gene (DTNBP1) and schizophrenia in 488 parent-offspring trios from Bulgaria. Biol Psychiatry 55: 971–975.
59. Fanous AH, van den Oord EJ, Riley BP, Aggen SH, Neale MC, et al. (2005) Relationship between a high-risk haplotype in the DTNBP1 (dysbindin) gene and clinical features of schizophrenia. Am J Psychiatry 162: 1824–1832.
60. Gornick MC, Addington AM, Sporn A, Gogtay N, Greenstein D, et al. (2005) Dysbindin (DTNBP1, 6p22.3) is Associated with Childhood-Onset Psychosis and Endophenotypes Measured by the Premorbid Adjustment Scale (PAS). J Autism Dev Disord 10: 1–8.
61. Millar JK, Wilson-Annan JC, Anderson S, Christie S, Taylor MS, et al. (2000) Disruption of two novel genes by a translocation co-segregating with schizophrenia. Hum Mol Genet 9: 1415–1423.
62. Millar JK, Christie S, Anderson S, Lawson D, Hsiao-Wei LD, et al. (2001) Genomic structure and localisation within a linkage hotspot of Disrupted In Schizophrenia 1, a gene disrupted by a translocation segregating with schizophrenia. Mol Psychiatry 6: 173–178.
63. Miyoshi K, Honda A, Baba K, Taniguchi M, Oono K, et al. (2003) *Disrupted-In-Schizophrenia 1*, a candidate gene for schizophrenia, participates in neurite outgrowth. Mol Psychiatry 8: 685–694.
64. Hattori T, Baba K, Matsuzaki S, Honda A, Miyoshi K, et al. (2007) A novel DISC1-interacting partner DISC1-Binding Zinc finger protein: implication in the modulation of DISC1-dependent neurite outgrowth. Mol Psychiatry 12: 398–407.

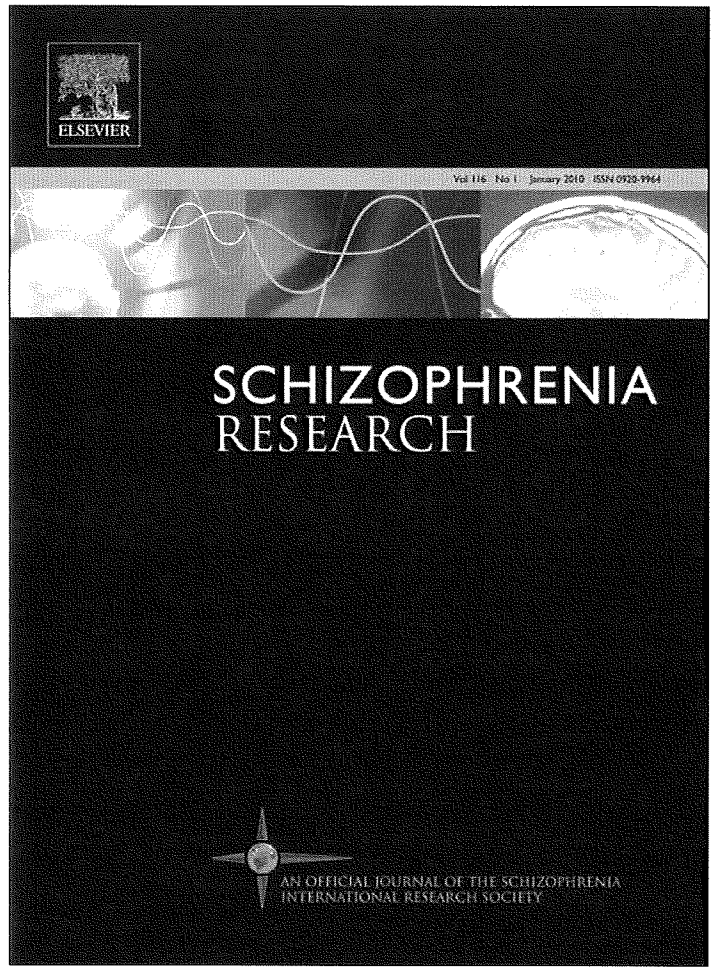

Schizophrenia Research 116 (2010) 61–67

Contents lists available at ScienceDirect

Schizophrenia Research

journal homepage: www.elsevier.com/locate/schres

The *dopamine D3 receptor* (*DRD3*) gene and risk of schizophrenia: Case–control studies and an updated meta-analysis

Ayako Nunokawa [a], Yuichiro Watanabe [a,b,*], Naoshi Kaneko [a], Takuro Sugai [a], Saori Yazaki [c], Tadao Arinami [c], Hiroshi Ujike [d], Toshiya Inada [e], Nakao Iwata [f], Hiroshi Kunugi [g], Tsukasa Sasaki [h], Masanari Itokawa [i], Norio Ozaki [j], Ryota Hashimoto [k], Toshiyuki Someya [a]

[a] *Department of Psychiatry, Niigata University Graduate School of Medical and Dental Sciences, 757 Asahimachidori-ichibancho, Chuo-ku, Niigata 951-8510, Japan*
[b] *Health Administration Center, Niigata University, 8050 Ikarashi-ninocho, Nishi-ku, Niigata 950-2181, Japan*
[c] *Department of Medical Genetics, Doctoral Program in Social and Environmental Medicine, Graduate School of Comprehensive Human Sciences, University of Tsukuba, 1-1-1 Tennodai, Tsukuba, Ibaraki 305-8575, Japan*
[d] *Department of Neuropsychiatry, Okayama University, Graduate School of Medicine, Dentistry and Pharmaceutical Sciences, 2-5-1 Shikata-cho, Okayama 700-8558, Japan*
[e] *Seiwa Hospital, Institute of Neuropsychiatry, 91 Bentencho, Shinjuku-ku, Tokyo 162-0851, Japan*
[f] *Department of Psychiatry, Fujita Health University School of Medicine, Toyoake, Aichi 470-1192, Japan*
[g] *Department of Mental Disorder Research, National Institute of Neuroscience, National Center of Neurology and Psychiatry, 4-1-1 Ogawahigashi, Kodaira, Tokyo 187-8502, Japan*
[h] *Health Service Center, University of Tokyo, 7-3-1 Hongo, Bunkyo-ku, Tokyo 113-8655, Japan*
[i] *Schizophrenia Research Project, Tokyo Institute of Psychiatry, 2-1-8 Kamikitazawa, Setagaya-ku, Tokyo 156-8585, Japan*
[j] *Department of Psychiatry, School of Medicine, Nagoya University, 65 Tsurumai-cho, Showa-ku, Nagoya, Aichi 466-8550, Japan*
[k] *The Osaka-Hamamatsu Joint Research Center for Child Mental Development, Osaka University Graduate School of Medicine, D3, 2-2, Yamadaoka, Suita, Osaka, 5650871, Japan*

ARTICLE INFO

Article history:
Received 13 July 2009
Received in revised form 15 October 2009
Accepted 17 October 2009
Available online 7 November 2009

Keywords:
DRD3
Resequencing
Schizophrenia
Tagging SNP

ABSTRACT

The dopamine D3 receptor (DRD3) has been suggested to be involved in the pathophysiology of schizophrenia. *DRD3* has been tested for an association with schizophrenia, but with conflicting results. A recent meta-analysis suggested that the haplotype T–T–T–G for the SNPs rs7631540–rs1486012–rs2134655–rs963468 may confer protection against schizophrenia. However, almost all previous studies of the association between *DRD3* and schizophrenia have been performed using a relatively small sample size and a limited number of markers. To assess whether *DRD3* is implicated in vulnerability to schizophrenia, we conducted case–control association studies and performed an updated meta-analysis. In the first population (595 patients and 598 controls), we examined 16 genotyped single nucleotide polymorphisms (SNPs), including tagging SNPs selected from the HapMap database and SNPs detected through resequencing, as well as 58 imputed SNPs that are not directly genotyped. To confirm the results obtained, we genotyped the SNPs rs7631540–rs1486012–rs2134655–rs963468 in a second, independent population (2126 patients and 2228 controls). We also performed an updated meta-analysis of the haplotype, combining the results obtained in five populations, with a total sample size of 7551. No supportive evidence was obtained for an association between *DRD3* and schizophrenia in our Japanese subjects. Our updated meta-analysis also failed to confirm the existence of a protective haplotype. To draw a definitive conclusion, further studies using larger samples and sufficient markers should be carried out in various ethnic populations.

1. Introduction

The dopamine D3 receptor (DRD3) has been suggested to be involved in the pathophysiology of schizophrenia (for a

* Corresponding author. Department of Psychiatry, Niigata University Graduate School of Medical and Dental Sciences, 757 Asahimachidori-ichibancho, Chuo-ku, Niigata 951-8510, Japan. Tel.: +81 25 227 2213; fax: +81 25 227 0777.
E-mail address: yuichiro@med.niigata-u.ac.jp (Y. Watanabe).

0920-9964/$ – see front matter © 2009 Elsevier B.V. All rights reserved.
doi:10.1016/j.schres.2009.10.016

review, Schwartz et al., 2000). DRD3 has relatively strong affinity for both first- and second-generation antipsychotics (Sokoloff et al., 1990). Postmortem studies have revealed changes in the mRNA and protein levels of DRD3 in the brains of patients with schizophrenia (Gurevich et al., 1997; Meador-Woodruff et al., 1997; Schmauss et al., 1993). Altered levels of *DRD3* mRNA in blood lymphocytes of patients with schizophrenia have also been reported (Ilani et al., 2001; Vogel et al., 2004). *DRD3* is located on 3q13.3 where some linkage analyses have suggested a region of susceptibility to schizophrenia (Brzustowicz et al., 2000; Kaneko et al., 2007). Therefore, *DRD3* is a promising functional and positional candidate gene for schizophrenia.

More than 60 studies have tested an association between *DRD3* and schizophrenia (Allen et al., 2008). The most extensively investigated *DRD3* polymorphism is Ser9Gly (rs6280) in exon 2 resulting in a serine to glycine substitution at codon 9. This polymorphism has been reported to be associated with altered dopamine binding affinity, suggesting that the Ser9Gly polymorphism may be functional (Lundstrom and Turpin, 1996). An initial study reported an association between homozygosity of this polymorphism and schizophrenia (Crocq et al., 1992). Some studies showed an association of the Ser allele with schizophrenia (Ishiguro et al., 2000; Shaikh et al., 1996), whereas others reported that the Gly allele was over-represented in patients with schizophrenia (Kennedy et al., 1995; Utsunomiya et al., 2008). However, two recent large meta-analyses did not provide evidence for an association between the Ser9Gly polymorphism and schizophrenia (Allen et al., 2008; Ma et al., 2008). Therefore, if *DRD3* is implicated in genetic susceptibility to schizophrenia, this cannot be wholly accounted for by the Ser9Gly polymorphism. This view has been supported by two studies using tagging single nucleotide polymorphisms (SNPs) based on linkage disequilibrium (LD) (Domínguez et al., 2007; Talkowski et al., 2006). A recent meta-analysis showed that the second most common haplotype (T–T–T–G) for the SNPs rs7631540–rs1486012–rs2134655–rs963468 was less frequent in patients with schizophrenia than in control subjects, suggesting that this haplotype may confer protection against schizophrenia (Costas et al., 2009).

Almost all previous studies on the association between *DRD3* and schizophrenia have been performed using a relatively small sample size and a limited number of markers. Here, we tried to increase the power by increasing the sample size and testing more markers, including tagging SNPs selected from the HapMap database and SNPs detected through resequencing of whole exon regions of *DRD3*. First, we conducted a moderate-scale case–control association study (595 patients and 598 controls) using 16 genotyped SNPs and 58 imputed SNPs that have not been directly genotyped. Second, we carried out an independent large-scale case–control association study (2126 patients and 2228 controls) to confirm the results of the first study, specifically to test the association of the haplotype T–T–T–G for the SNPs rs7631540–rs1486012–rs2134655–rs963468 with schizophrenia. Third, we performed an updated meta-analysis of this haplotype to assess the collective evidence across individual studies.

2. Materials and methods

The present study was approved by the Ethics Committee of each participating institute, and written informed consent was obtained from all participants. All participants were unrelated Japanese subjects.

2.1. Subjects

The first population consisted of 595 patients with schizophrenia (313 men and 282 women; mean age, 40.2 [SD 14.1] years) and 598 control subjects (311 men and 287 women; mean age, 38.1 [SD 10.5] years). These subjects partially overlapped with those in the report of Tanaka et al. (1996). Case and control groups were matched for sex ($p=0.836$). Although the mean age of the patients was significantly higher than that of the control subjects ($p=0.004$), the difference in mean age between the groups was relatively small (2.1 years). The second population consisted of 2126 patients with schizophrenia (1137 men and 989 women; mean age, 47.3 [SD 14.3] years) and 2228 control subjects (1189 men and 1039 women; mean age, 46.6 [SD 13.9] years). Case and control groups were matched for sex ($p=0.940$) and age ($p=0.083$).

We conducted a psychiatric assessment of every participant, as described previously (Nunokawa et al., 2007). In brief, the patients were diagnosed according to the *Diagnostic and Statistical Manual of Mental Disorders Fourth Edition* (DSM-IV) criteria by at least two experienced psychiatrists, on the basis of all available sources of information, including unstructured interviews, clinical observations and medical records. The control subjects were mentally healthy subjects with no self-reported history of psychiatric disorders; they showed good social and occupational skills, but were not assessed using a structured psychiatric interview.

The subjects for resequencing of exon regions were six patients with schizophrenia from a Japanese single multiplex schizophrenia pedigree. In this pedigree, our previous linkage analysis revealed that 3q is one of the candidate regions for schizophrenia (Kaneko et al., 2007). These patients were diagnosed according to the DSM-IV criteria by two experienced psychiatrists, on the basis of all available sources of information, including direct interviews using the Structured Clinical Interview for DSM-IV Axis I disorders and Axis II disorders, medical records, and information from reliable relatives and psychiatric professionals.

2.2. Tagging SNP selection

Tagging SNPs for *DRD3*, covering gene region and the 5′ and 3′ flanking regions (chr3:115307882..115402406), were selected from the HapMap database (release#22, population: Japanese in Tokyo [JPT], minor allele frequency [MAF]: more than 0.05). We applied the criterion of an r^2 threshold greater than 0.8 in the *'aggressive tagging: use 2- and 3-marker haplotype'* mode using the 'Tagger' program (de Bakker et al., 2005), as implemented in Haploview v4.0 (Barrett et al., 2005); rs6280 (Ser9Gly) was forced to be selected as a tagging SNP. To confirm the existence of a common protective haplotype (Costas et al., 2009), we also included rs963468.

2.3. Resequencing of exon regions

All seven exons of *DRD3* were screened for polymorphisms using direct sequencing of PCR products. The sequences